PROCEEDINGS

OF THE

KSEEE-JSAEM 2013 INTERNATIONAL ENGINEERING CONFERENCE

ON

4th-5th SEPTEMBER, 2013

AT

DEDAN KIMATHI UNIVERSITY OF TECHNOLOGY

NYERI, KENYA

SUPPORTED BY:

Kenya Society of Electrical & Electronic Engineeers

JSAEM The Japan Society of Applied Electromagnetics and Mechanics

Jomo Kenyatta University of Agriculture and Technology

Design Optimization of a Renewable Hybrid Energy System

J. O. Obasi[1], L. M. Ngoo[2] and C. M. Muriithi[3]
[1]Electrical & Electronic Engineering Department, JKUAT
[2]Multimedia University of Kenya
[3]Electrical & Electronic Engineering Department, JKUAT
[1]jayobasi@gmail.com, [2]mwalungoo@yahoo.com, [3]cmaina77@yahoo.com

Abstract-This paper proposes the optimal design of a renewable hybrid energy system consisting of solar, wind energy with battery storage suitable for application in remote areas. The study investigates the possibility of reducing the overall size of a system already installed in a school in Maji Mazuri, Kiserian. The main aim of the study is to reduce size of the renewable systems and reduce energy storage. The study investigates the effects of reducing load demand on the size of the system components. DC LED lamps are proposed for all the lighting needs of the school in order to reduce the load demand especially during peak hours. The results show that the optimized system is able to meet the load demand. Homer software is used in the design and optimization of the renewable hybrid power system.

Keywords- Homer, Hybrid Energy System, Solar, Wind.

I. INTRODUCTION

With increasing concern on global environmental pollution and increased cost of electricity, hybrid energy systems based on renewable energy are now playing a key role in meeting current electricity demand. However, power produced from renewable sources such as solar PV and wind energy system is highly variable due to their intermittent nature. This poses serious technical and economic challenges when designing stand alone hybrid energy systems due to the uncertainties in the electricity generation. To provide balance between energy generation and load demand, energy storage systems are usually used [1]. Stand alone systems usually require large storage systems to cover for periods when there is no generation from the renewable resources [2]. Hybridizing solar PV and wind due to their complementary nature improves the system reliability and can significantly reduce the storage requirements [3] [4] [5].

A major challenge in the design of renewable resources is their intermittent nature which results in excess capacity and shortages. The challenge is reducing the shortages and excesses while ensuring the quality of supply [6]. Optimizing the size of the solar PV, wind generator and battery will improve the system reliability as well as reduce the overall cost of the system. Optimal sizing methods for standalone hybrid energy systems can either be single objective or multi-objective. In single objective the main aim is to ensure reliable supply while keeping the cost of the system at a minimum. In multi-objective optimization, the power supply reliability, the overall cost of the system and environmental considerations such as pollutant emissions are taken into account.

This paper proposes an optimal sizing method for an existing PV/wind/battery hybrid energy system by minimizing excess capacity and energy storage. The system was sized to meet all demand especially during peak hours, resulting in an oversized system. During mid-afternoon when the sun is overhead the power generated by PV exceeds the load demand, battery charging power and dump load power. The same case applies for the wind generator although the timing varies with the availability of wind. This paper proposes peak shaving by replacing all lighting loads with D.C. LED bulbs. LED lamps offer extraordinary power saving compared to fluorescent, compact fluorescent lamps and halogen lamps while giving the same light output.

II. ENERGY DEMAND AND RESORCES

A: Load demand

The objective of this study was to optimize the design of a renewable hybrid energy system by reducing excess capacity from the renewable resources. Maji Mazuri School in Kiserian, Kajiado County has been selected for study as it already has an existing system with a lot of excess electricity. Kajiado borders Nairobi to the South and lies in the expansive Great Rift Valley. The electrical load for the school is mainly for

lighting, electrical appliances such as radio, T.V, computers and water pumping. Daily load demand is illustrated in Fig 1.

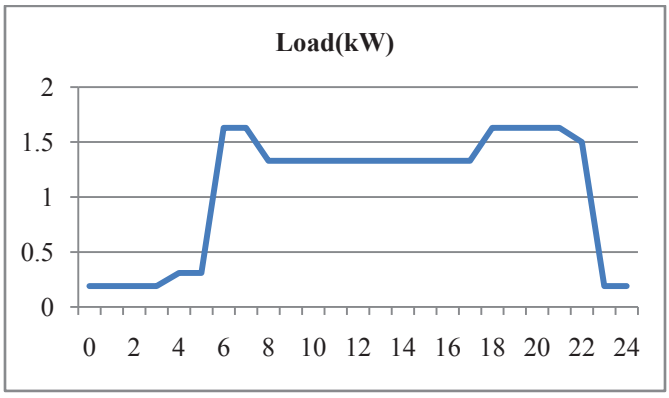

Fig. 1 Daily Load Profile

There are two peaks, one occurring between 6 and 8 am in the morning and 7 and 10pm in the evening.

B: Solar Radiation

Solar energy is a promising renewable energy resource because of its unlimited potential and availability. Solar radiation is determined by the location on the earth's surface, the season and time of day. Monthly averages of solar radiation was collected from the Kenya Meteorological Department and used as inputs to the Homer software. Monthly averages for the solar radiation for the year are illustrated in Fig. 2. The scaled annual average clearness index is 0.55 and daily radiation is 5.508 kWh/m^2.

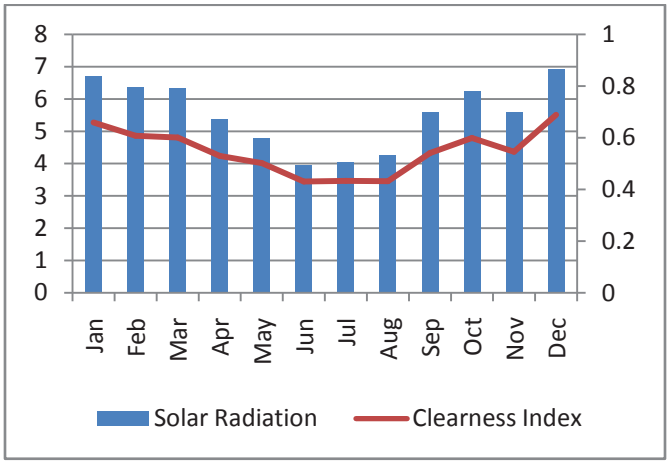

Fig. 2 Monthly average Solar Radiation

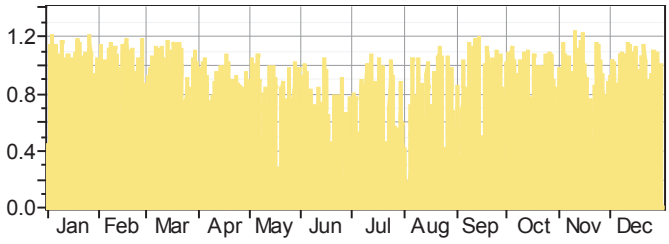

Fig. 3 Annual horizontal solar radiation

C: Wind Resources

Wind energy is the fastest growing among renewable energy technologies. The annual monthly wind speeds are shown in Fig. 3. Wind speeds suitable for power generation are observed between the months of Jan to May and Sep to Dec. The period between May and Aug on average there is very little wind speed about 3m/s which results in very low output from the wind generator.

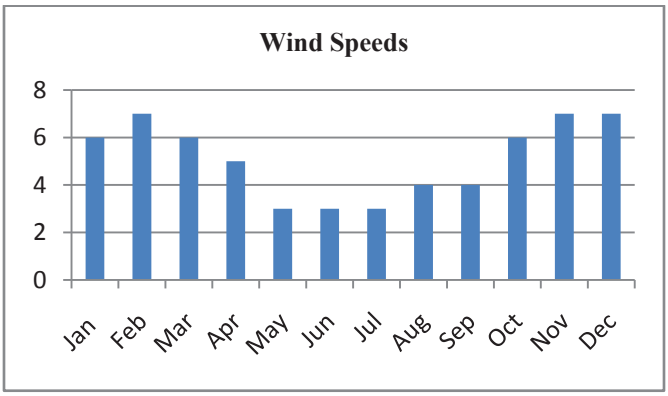

Fig. 3 Monthly average Wind Speeds

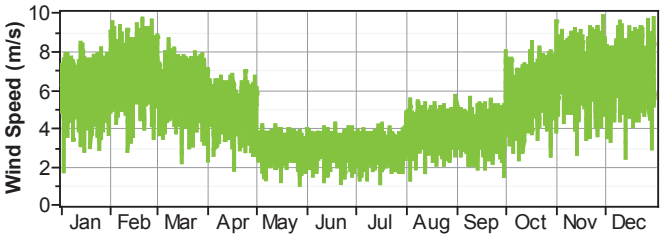

Fig. 4 Annual wind speeds

III. METHODOLOGY

This study seeks to optimize an existing hybrid energy system integrating wind energy, solar PV and batteries. The existing system consists of a 3.6 kW solar array, a 6 kW wind turbine and 30 batteries rated at 12v and 200Ah. The system is characterized by excess capacity

which cannot be utilized especially around midday resulting to a lot of wasted energy.

In order to optimize the system this study proposes to separate the loads into AC and DC, this will reduce the peak load due to a.c. lighting requirements. All electric appliances will be served by AC and all lighting will be replaced by DC LED lamps. LED lamps offer extraordinary power saving compared to fluorescent, compact fluorescent lamps and halogen lamps while giving the same light output. LED lamps rated 3watts have been chosen to replace the existing fluorescent and compact fluorescent lamps. Desktop computers have also been replaced with laptop computers while television sets have also been replaced with LCD televisions sets to reduce power consumption.

The new energy demand for the school is illustrated in the following figures

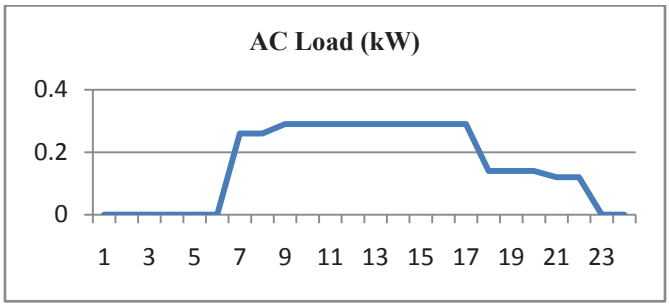

Fig. 5 Daily a.c load profile

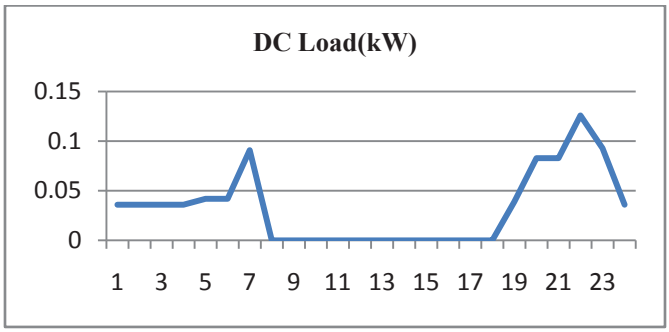

Fig.6 Daily d.c. load profile

The major components for the hybrid power system are solar PV panels, wind turbines, power converter and batteries. Solar panels are the primary source of power while the wind turbines and batteries provide electricity during periods of no generation from the solar panels. Homer requires the number of units to be considered, the capital costs, replacement costs, operation and maintenance costs and the lifetime of the components to simulate the system. The figure below shows the considered hybrid energy system.

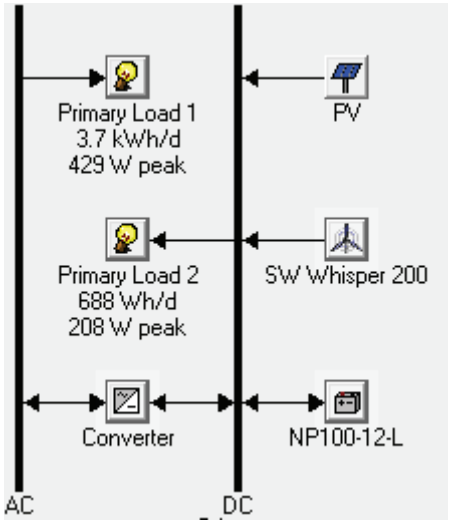

Fig. 7 Hybrid Energy System

The main aim of optimizing the system is to find the optimal decision variables of the system components that will match the load to the available wind and solar resources throughout the year. The various decision variables in the system to consider include:

- The size of the PV array
- The number of wind turbines
- The size of the converter
- The number of batteries

A. Solar Array

The Kyocera KD250GX-LFB 250 watt solar panel is considered for this study with one unit costing 375 dollars. The operation and maintenance costs are practically zero and the lifetime of the system is taken to be 25 years.

B. Wind Turbine

The 1kW DC SW Whisper 200 wind turbine with initial capital cost of 3,000 dollars is considered. The lifetime of the wind turbine is taken as that of the system to be 25 years.

C. Power converter

A power converter is required to convert DC to AC. A converter of 2.5kW is considered costing 950 dollars. The lifetime of the power converter is 25 years.

D. Batteries

Batteries are used in the hybrid power system to provide electrical power when there is little or no output from renewable resources. Batteries will supply electrical power when the renewable energy resources cannot meet the load requirements. The Dayliff Champion 12V 100Ah battery is considered in this study. Each battery costs 250 dollars and has an expected lifetime of about six years.

IV. RESULTS AND DISCUSSION

From the simulation the configuration containing one Whisper 200 1 kW wind turbine, 1.25 kW array, 10 batteries and 2.5kW inverter is found to be the optimum configuration. The optimized system is smaller in size compared to the existing system as shown in the following table.

Table 1: Comparison of designed systems

System	PV array	Wind Turbine	Batteries
Existing	3.6 kW	6 kW	30
optimized	1.25 kW	1kW	10

The Power generated from the wind generator and solar PV is sufficient for the better part of the year except during the months of May, June and July when the power generated is lower. The figure below shows the contribution of Solar PV and Wind energy resources to the total electricity production throughout the year.

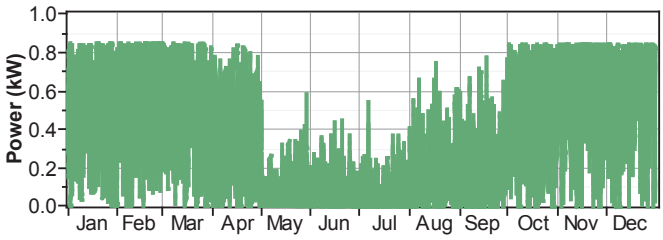

Fig. 8 Annual Wind Turbine Power

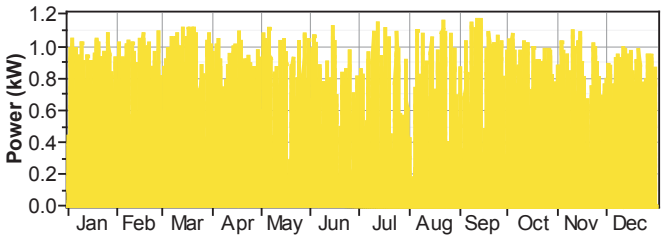

Fig. 9 Annual solar PV power

Batteries provide power during periods of little or no generation from the wind and solar generators. From the simulation the batteries operate optimally for most part of the year except during the months from May to September. The following figures show the batteries input power and state of charge (soc) throughout the year.

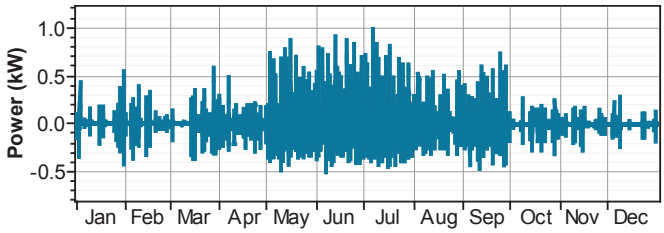

Fig. 10 Battery input power

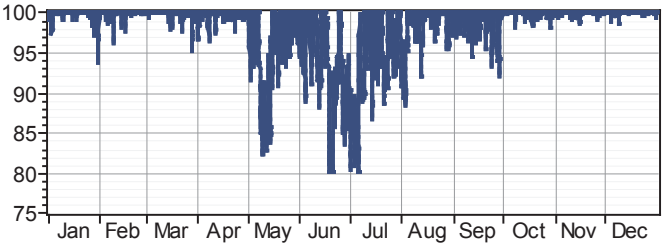

Fig. 11 Battery state of charge (%)

Between the months of May and September power from the renewable is reduced and the batteries have to be used regularly to provide power. There is also very little power generated such that the batteries are sometimes used to the lowest allowable SOC which is 80%.

Table 2: Comparison of Capital Cost

	Existing ($)	Optimized ($)
PV array	5,184	1.850
Wind Turbine	5,800	3,000
Batteries	4,200	2,500
Inverter	2,420	950
Capital cost	17,604	8,300

From the results the optimized system is cheaper by about 9,300 dollars. This is due to the reduced size of PV array, number of batteries, size of inverter and the size of wind turbine. The total cost of replacing the bulbs with LED bulbs, computers and television sets is about 6,245 dollars. The total savings realized is about

3,000 dollars. However, this does not include the salvage value of all the items being replaced.

V. CONCLUSION

Most remote areas are not connected to the grid because of the high costs involved in grid extension. Hybrid energy systems offer a promising alternative for electrification of these areas. The systems integrate locally available renewable resources with battery storage to ensure grid quality electricity supply.

From the simulation results a Solar-wind-Battery system consisting of a 1.25 kW solar array, one wind turbine, 10 batteries and a 2.5 kW inverter is found to be the optimum system. The system is able to reliably meet the load demand throughout the year and reduce excess capacity.

The analysis of results shows significant contribution of solar PV and wind turbines. Batteries are extensively employed between the months of May to September when the output from renewable sources is low.

Significant cost savings are realized by optimizing the system by reducing the peak loads which are associated with lighting and a.c appliances. This shows that demand side management can significantly reduce the load demand and thus reduce the overall size of the system.

ACKNOWLEDGEMENT

The authors would like to thank the National Commission for Science and Technology (NCST) of Kenya for their support in this project.

References

[1] Yuri V. M., Pengwei D, Michael C. W., and Chunlian J and Howard F. I, "Sizing Energy Storage to Accommodate High Penetration of Variable Energy Resources," *IEEE trans on Sustainable Energy*, vol. 3, no. 1, pp. 34-40, January 2012.

[2] Ruan X, Mao C, Zhang B and Luo Y Xu L, "An Improved Optimal Sizing Method for Wind-Solar-Battery Hybrid Power System," *IEEE Transactions on Sustainable enrgy Energy*, vol. 4, no. 3, pp. 774-785, March 2013.

[3] Perez E, Aparicio N and Rodriguez P Beltran H, "Daily Solar Energy Estimation for Minimizing Energy Storage Requirements in PV Power Plants," *IEEE Trans. Sustainable Energy*, vol. 4, no. 2, pp. 474-481, April 2013.

[4] Dong H and Xiaokang L Xiangjun L, "Battery Energy Storage Station (BESS)-Based Smoothing Control of Photovoltaic (PV) and Wind Power Generation Fluctuations," *IEEE Trans. Sustainable Energy*, vol. 4, no. 2, pp. 464-473, March 2013.

[5] Key Pour R, Shajari s, "Reduction of energy storage system for smoothing hybrid wind-PV power fluctuation," in *IEEE Conference Preceedings*, 2012, pp. 115-117.

[6] K. Suomalainen, C. Silva, and P. Ferrão and S. Connors, "Wind power design in isolated energy systems: Impacts of daily wind patterns," *Elsevier*, vol. 1, no. 1, pp. 533-540, 2013.

Static Voltage Stability Assessment of Nairobi Area Power Distribution Network

Oketch S.A[1], Muriithi C.M[2], Kaberere K.K[3]

Dept. of Electrical & Electronic Engineering, Jomo Kenyatta University of Agriculture & Technology
P.O. Box 62000, Nairobi, Kenya

[1]engsoketch@yahoo.com,[2]cmmuriithi@eng.jkuat.ac.ke,[3]kkkanuthu@eng.jkuat.ac.ke

Abstract-**The Nairobi Area Power distribution network supplies over 50% of Kenya's national load demand. The increase in load demand in the network, over the years has generated interest to the network's voltage stability status. Voltage stability is an important factor that needs to be taken into consideration during the planning and operation of power systems in order to avoid voltage collapse and subsequently partial or full system blackout. The study of the voltage stability characteristics can provide a way to prevent this event from happening.**

This paper presents a study to assess the voltage stability of Nairobi Area Power distribution network using static analyses methods. The network power flow problem is formulated, and solution attained using Newton Raphson method to determine the base operating voltages and angles, the power flows, and to compute the full Jacobian matrix. The Sensitivity and Modal analyses methods are used to investigate the network weak buses and branches, and to analyse the response of network generators to incremental changes in reactive loadings. In the rest of this works, the P-V and Q-V curves analysis methods are used to compute the active and reactive power margins respectively, of the identified weak buses. The analysis is performed to simulate the peak loadings conditions of June, 2012

.

Keywords— **Voltage stability, Sensitivity analysis, Modal analysis, Active power Margins and Reactive power margins.**

I. INTRODUCTION

In the last few years the need to increase the transfer capacity of the existing distribution networks without major investments and also without compromising the security of the power system has led to a situation where utilities operate power systems relatively closer to voltage stability limits [1].

The continued growth in load demand or contingency in the network may lead to a state of voltage instability, and eventually, voltage collapse.

Voltage stability is concerned with the ability of power system to maintain acceptable voltages at all buses under normal conditions and after being subjected to a disturbance [2]. Voltage stability can be attained by sufficient generation and transmission of energy. Generation and Transmission have definite capacities that are peculiar to them and should not be exceeded in a healthy power system. The main factor causing voltage instability is the inability of the power system to meet the demand for the reactive power in a heavily stressed system
[2], [3].

Therefore a power system is said to experience voltage instability when a disturbance or sudden increase in load demand or change in system conditions causes a progressive and uncontrollable decline in voltage levels. Voltage collapse refers to the process by which the sequence of events leading to voltage instability leads to low unacceptable voltages in a significant part of the power system [2]. It is the result of accumulative processes involving the actions and interactions of many devices, controls and protective systems.

Most utilities now consider Voltage stability in their planning and operation of the power systems in order to avoid voltage collapse and subsequently partial or full system blackout.

A number of techniques are available in literature for the analysis of voltage stability. These techniques are based on either steady state and/or dynamic analysis methods [2]. Since the system dynamics that influence voltage stability are usually slow, many aspects of the problem can be effectively analysed using static methods, which examine the viability of the equilibrium points represented by a specified operation of the power system. Static analysis methods, in addition to providing information with regard to the sensitivity or degree of stability, also involves the computation of only algebraic equations and are thus efficient and faster.

This paper presents an assessment of the voltage stability of the Nairobi Area Power Distribution Network using static analyses approaches. The power flow problem for the network configuration was formulated and solution attained by Newton

Raphson method, using a MATLAB based program. The VQ sensitivity and QV modal analyses methods are employed to investigate the network weak buses and branches, and also the response of the network generators to the incremental changes in reactive loadings. The buses identified as weak are further investigated by analysing their P-V and Q-V curve characteristics on PowerFactory DIgSILENT software, to determine their active and reactive power margins respectively. The analysis is performed to simulate the peak loading conditions of June, 2012.

The paper is organized as follows: Section I served as introduction. In section II we discuss the voltage stability analysis, section III presents a case study using the Nairobi Area Power Distribution Network, and in IV we outline conclusions and recommendations.

II. VOLTAGE STABILITY ANALYSIS

The linearized steady state system power voltage equations are presented by [2], [4]:

$$\begin{bmatrix}\Delta P\\ \Delta Q\end{bmatrix}=\begin{bmatrix}J_1 & J_2\\ J_3 & J_4\end{bmatrix}\begin{bmatrix}\Delta\delta\\ \Delta V\end{bmatrix} \qquad (1)$$

Where ΔP and ΔQ are the mismatch active and reactive powers, ΔV and $\Delta\delta$ are the unknown voltage and angle correction vectors, and

$\begin{bmatrix}J_1 & J_2\\ J_3 & J_4\end{bmatrix}$ - is the network full Jacobian matrix.

A. *Q-V Sensitivity Analysis*

The elements of Jacobian matrix give the sensitivity between the power flows and bus voltage changes [2], [5], [6].The system voltage stability is affected by both P and Q. However at each operating point if P is kept constant then voltage stability is evaluated by considering incremental relationship between Q and V.

Based on these considerations then, in equation (1) if $\Delta P = 0$, then

$$\begin{bmatrix}0\\ \Delta Q\end{bmatrix}=\begin{bmatrix}J_1 & J_2\\ J_3 & J_4\end{bmatrix}\begin{bmatrix}\Delta\delta\\ \Delta V\end{bmatrix} \qquad (2)$$

$$\Delta Q = \left[J_4 - J_3 J_1^{-1} J_2\right]\Delta V \qquad (3)$$

$$\Delta Q = J_R \Delta V \qquad (4)$$

$$J_R = \left[J_4 - J_3 J_1^{-1} J_2\right] \qquad (5)$$

J_R - is the reduced Jacobian matrix of the system.

From equation (4),

$$\Delta V = J_R^{-1}\Delta Q \qquad (6)$$

The matrix J_R^{-1} is the reduced V-Q Jacobian and its i^{th} diagonal element is the sensitivity at bus i.

The V-Q sensitivity at a bus represents the slope of Q-V curve at a given operating point. A positive V-Q sensitivity is indicative of stable operation; the smaller the sensitivity the more stable the system]. As the stability decreases, the magnitude of the sensitivity increases, becoming infinite at the stability limit. Conversely a negative sensitivity is indicative of unstable operation. A small negative sensitivity represents a very unstable operation [2], [7], [8], [9].

B. *Q-V Modal Analysis*

Voltage stability characteristics of the system can be identified by computing the eigenvalues and eigenvectors of the power flow (reduced) Jacobian matrix, J_R [2], [3], [5], [7], [9].

Let $J_R = \xi\Lambda\eta$ (7)

Where

ξ =Right eigenvector of matrix J_R

η =Left eigenvector of matrix J_R

Λ =diagonal eigenvalue of matrix J_R

From equation (7),

$$J_R = \xi\Lambda^{-1}\eta \qquad (8)$$

Incremental changes in reactive power and voltage are related by equation (6). Substituting equation (8),

$$\Delta V = \xi\Lambda^{-1}\eta\Delta Q \qquad (9)$$

Or

$$\Delta V = \sum_i \frac{\xi_i \eta_i}{\lambda_i} \Delta Q \qquad (10)$$

Where

λ_i - is the i^{th} eigenvalue

ξ_i - is the i^{th} right eigenvector of J_R

η_i -is the i^{th} row left eigenvector of J_R

Each eigenvalue λ_i and the corresponding right and left eigenvectors ξ_i and η_i define the i^{th} mode of V-Q response.

Since $\xi^{-1} = \eta$ equation (9) can be written as:

$$\eta \Delta V = \Lambda^{-1} \eta \Delta Q \qquad (11)$$

Or

$$v = \Lambda^{-1} q \qquad (12)$$

Where

$v = \eta \Delta V$ is the vector of modal voltage variations, and

$q = \eta \Delta Q$ is the vector of modal reactive power variations

The i^{th} modal voltage variation can therefore be written as:

$$v_i = \frac{1}{\lambda_i} q_i \qquad (13)$$

From equation (13) the stability of mode i with respect to reactive power changes is defined by the modal eigenvalue λ_i . Large values of λ_i suggest small changes in modal voltage for reactive power changes. As the system is stressed the value of λ_i becomes smaller and the modal voltage becomes weaker. If the magnitude of λ_i is equal to zero, the corresponding modal voltage collapses since it undergoes infinite changes for reactive power changes. A system is therefore defined as stable if all the eigenvalues of J_R are positive. The bifurcation or voltage stable limit is reached when at least one eigenvalue reaches zero; that is one or more modal voltages collapses. If any of the eigenvalues is negative the system is unstable. The magnitudes of eigenvalues provide a relative measure of the proximity of the system to instability.

1) Bus Participation Factors: The left and right eigenvectors corresponding to the critical mode in the system can provide information concerning voltage instability, by identifying the elements participating in these modes. The relative participation of bus k in mode i, is given by bus participation factor:

$$P_{ki} = \xi_{ki} \eta_{ik} \qquad (14)$$

Bus participation factors corresponding to the critical modes can predict nodes or areas in a power system susceptible to voltage instability. Buses with large participation factors to the critical mode correspond to the most critical of system buses. In practical systems with several thousand buses, there is usually more than one weak mode associated with different parts of the system, and the mode associated with the minimum eigenvalue may not be the most troublesome mode as the system is stressed [2].

2) Branch Participation Factors: If we assume vector of modal reactive power variations, q corresponding to mode i to have all elements equal to zero except the i^{th}, which equals to 1, then the corresponding vector of bus reactive power variations is

$$\Delta Q^{(i)} = \eta^{-1} q = \xi q = \xi_{(i)} \qquad (15)$$

Where ξ_i is the i^{th} right eigenvector of J_R

The vector of bus voltage variations is

$$\Delta V^{(i)} = \frac{1}{\lambda_i} \Delta Q^{(i)} \qquad (16)$$

The corresponding vector of bus angle variations is

$$\Delta \theta^{(i)} = -J_1^{-1} J_2 \Delta V^{(i)} \qquad (17)$$

The linear relationships for the real and imaginary powers at a bus can be obtained for small variations in variables θ and V by forming total differentials [10] as follows:

For a PQ bus bar

$$\Delta P_k = \sum_{m \in k} \frac{\partial P_k}{\partial \theta_m} \Delta \theta_m + \sum_{m \in k} \frac{\partial P_k}{\partial V_m} V_m \qquad (18)$$

$$\Delta Q_k = \sum_{m \in k} \frac{\partial Q_k}{\partial \theta_m} \Delta \theta_m + \sum_{m \in k} \frac{\partial Q_k}{\partial V_m} V_m \qquad (19)$$

For PV bus bar, only equation (18) is used since Q_k is not specified. For slack bus bar, no equation is used.

With angle and voltage variations for both the sending end and the receiving end known, the linearized change in branch reactive loss can be calculated [2].

The relative participation of branch j in mode i is given by the participation factor:

$$P_{ji} = \frac{\Delta Q_{loss} \text{ for branch j}}{\text{ma x imum } \Delta Q_{loss} \text{ for all branches}} \quad (20)$$

Branch participation factor indicates for each mode which branches consume the most reactive power in response to an incremental change in reactive load. Branches with high participations are either weak links or are heavily loaded [2].

3) Generator Participation Factor: The relative participation of machine m in mode i, is given by generator participation factor [2].

$$GPF_{m.i} = \frac{\Delta Q_m \text{ for machine m}}{\text{max imum } \Delta Q \text{ for all machines}} \quad (21)$$

The generator participation factor indicates for each mode which generator supply most reactive power in response to an incremental change in system reactive loading.
Generator Participation factors provides important information regarding proper distribution of reactive reserves among all machines.
Generators with high $GPF_{m.i}$ are important in maintaining stability of mode i [2].

C. *P-V and Q-V curves Analysis*

At the voltage collapse point, the maximum power transfer limit has been reached, and therefore operation of power system faces difficulties. For a satisfactory operation, a sufficient power margin must be allowed [2]. In assessing the network proximity to voltage collapse point, P-V and Q-V curves are plotted and analysed.
It has been argued in literature that Q-V curve technique is preferable when determining the reactive supply problems, whereas the P-V curve analysis is preferable for providing power loading and transfer indications [11].

1) P-V Curves: The P-V curves have been used widely for predicting the margins of voltage stability. For a given value of active power, there are two possible voltages (higher voltage with lower current or lower voltage with higher current). The normal operation corresponds to higher voltage solution [2], [9], [12], [13].

The P-V curve at a load bus is produced by incrementally increasing the active power, P and performing series of power flow solutions for the different loading levels, until the maximum power transfer limit is reached.

The P-V curve is plotted using the calculated values of voltages corresponding to the incremental changes of P values at the candidate bus. A typical P-V curve is shown in Fig 2.1

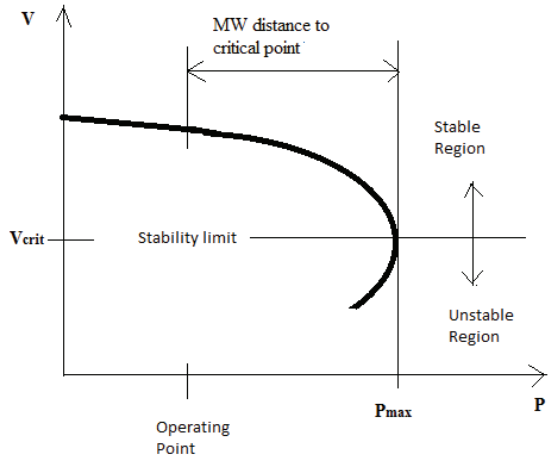

Fig. 2.1: Typical (P-V) Curve

As shown in Fig 2.1 the real power margin at a load bus is the Megawatt (MW) distance from the operating point to the voltage collapse point.

2) Q-V Curves: The Q-V relationship represents the sensitivity and variation of a bus voltage with respect to reactive power injections or absorptions [2]. A system is voltage stable if V-Q sensitivity is positive for every bus and voltage unstable if V-Q sensitivity is negative for at least one bus.

The Q-V curves are used by many utilities for determining proximity to voltage collapse so that operators can make good decision to avoid losing system stability [11].

The Q-V curves are produced by incrementally increasing the reactive power demand, Q at the candidate bus, and running series of power flows with each change until the power system is not able to meet the demand for the reactive power.

A typical Q-V curve is shown in Fig. 2.2. As seen in the figure, the Reactive Power Margin is the Mega Volt Ampere reactive (MVAr) distance from the operating point to the critical voltage.

III. CASE STUDY

Figure 1 shows the single line diagram of the Nairobi Area supply distribution network. It consists of 66kV radial distribution lines originating from four bulk power supply points. Rings of transmission lines at 132kV and 220kV supplies the bulk supply points from six hydroelectric and two geothermal power stations. The network also has two Diesel generators and one small hydroelectric power plants injecting power at 66kV.

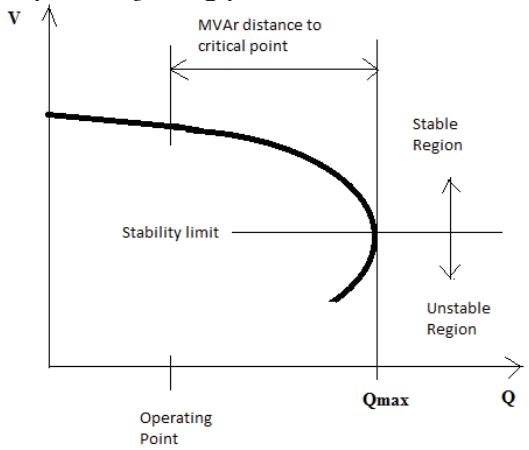

Fig.2.2: Typical (Q-V) Curve

Apart from the 66kV voltage level, the distribution network has other voltage levels: 33kV, 11kV and the low voltages. But this study is mainly on the 66kV network.

A. *Network voltage operating conditions*

The power flow problem was formulated and solved by Newton Raphson method using a MATLAB based program to obtain the operating voltages and angles, line flows and the full Jacobian matrix.

The voltage variation criteria in Kenya are +/- 6% for distribution networks and +/- 10% for transmission networks [14]. Table I of section IV shows buses operating outside this criterion.

B. *Q-V Sensitivity analysis*

The MATLAB program further computed the Reduced Jacobian and the reduced V-Q Jacobian matrices from the full Jacobian matrix.

The sensitivity factors of the load buses are evaluated from the diagonal elements of the reduced V-Q Jacobian matrix. Figure 2 of section IV shows the buses with highest sensitivity factors in the network.

C. *Q-V Modal analysis*

The MATLAB program was used to compute the eigenvalues, the right and left eigenvector matrices of the reduced Jacobian matrix, from which the bus and branch participation factors were evaluated.

Table III and IV of section IV shows the smallest modal eigenvalues for the network operating condition.

Figure 3 of section IV shows buses with highest bus participation factors for the network operating condition.

Figures 4 of section IV shows the branches with highest branch participation factors in the network.

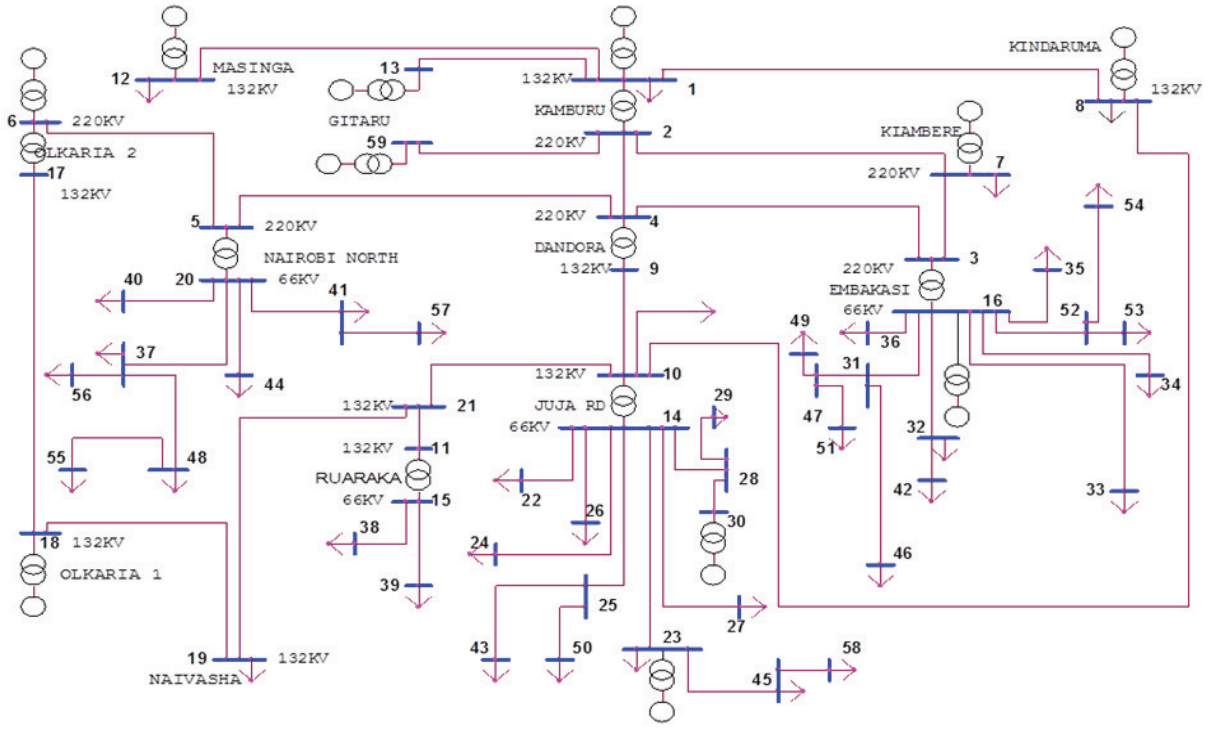

Figure 1: Nairobi Area Power Supply Distribution Network as at July, 2012.

Figures 5 of section IV shows the generator buses with highest generator participation factors in the network.

D. *Determination of Active Power Margins.*

The P-V curves in this research were plotted in PowerFactory DIgSILENT software, after modelling the network shown in Fig 1. The plotting is done by the software based on the principles outlined in section II.

The real power margin is calculated by subtracting the P value at the base operating point from the maximum permissible real power, P_{max} , which is at the collapse point, as illustrated in Fig 2.1 of section II.

Figure 6 of section IV shows the P-V curves for the buses considered weak in the network.

E. *Determination of reactive Power margins*

The data for plotting the Q-V curves were obtained by recording the reactive power demands corresponding to active power increments in part D, until the maximum loading limit is reached.

The reactive power margin, Q is computed by subtracting the Q values at the operating point from the maximum reactive power, Q_{max} which is at the maximum loading limit, as is illustrated in section II. Figure 7 of section IV shows the Q-V curves of the buses considered weak in the network.

IV. Results and Analysis

The buses which are operating outside the recommended voltage criteria are shown in Tables I.

TABLE I
BUSES OPERATING OUTSIDE VOLTAGE CRITERIA

BUS	27	29	42	51	55
VOLT. (P.U)	0.913	0.932	0.936	0.938	0.927

Figure2 shows the buses with the largest Q-V sensitivity factors for the network. Buses with high sensitivity factors are comparatively weaker in the network. The study shows buses 42(Magadi), 55 (Karen), 27 (EPZ) and 48 (Kikuyu) are the most sensitive buses in the network, and therefore weak nodes.

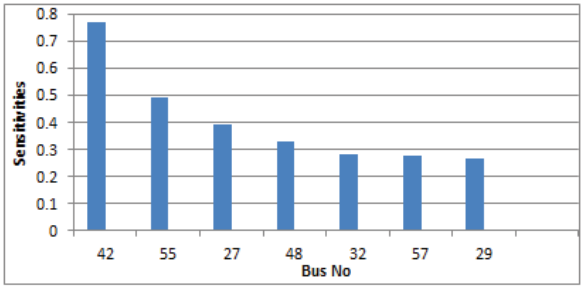

Fig2: Largest Bus sensitivity Factors

Tables II shows the magnitudes of smallest modal eigenvalues. The magnitude of the smallest eigenvalue gives indication of the network proximity to voltage collapse.

TABLE II
THE SMALLEST EIGENVALUE

MODE	30	39	40	33	34	32	31	35
EIGENVALUE	0.7	1.1	2.2	2.6	2.6	3.1	3.3	5.3

Figure3 shows buses with dominant bus participation factors. Buses with high participation factors are weak nodes in the network. The study shows buses 55(Karen), 48(Kikuyu), 56(KPC Ngema) and 57(Gigiri W/Works) are the weak nodes in the network.

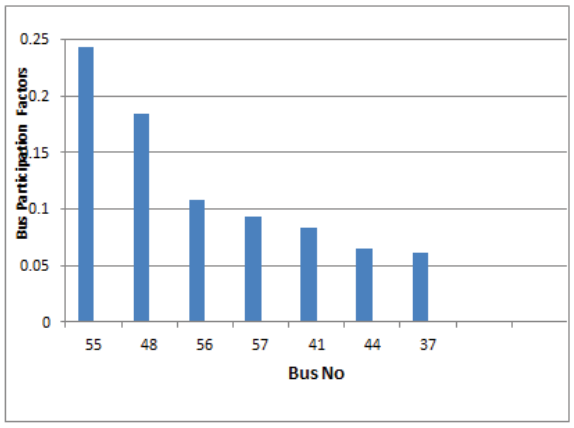

Fig. 3: Largest Bus Participation Factors

Figure 4 shows the network branches which have dominant participation factors. Branches with higher participation factors are weak links in the network. They are either overloaded or consumers of most reactive power. The study shows branches 37-48(Limuru-Kikuyu), 37-20(Limuru-Nairobi North) and 48-55 (Kikuyu-Karen) are the weak links in the network.

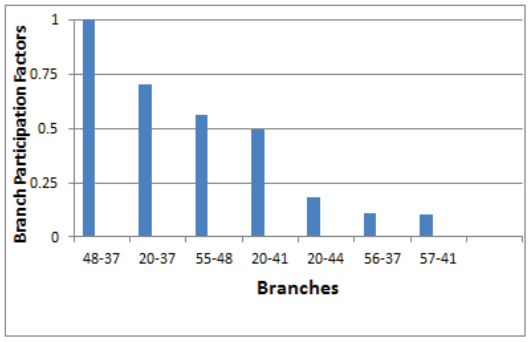

Fig. 4: Largest Branch Participation Factors

Figure 5 shows generator buses with the highest Generator participation factors. The Generators participation factors indicate for each mode, which generators supply the most reactive power in response to the system incremental reactive power loadings. The result shows that generators 6 (Olkaria II) and 7 (Kiambere) have the highest participation factors. These generators are important in maintaining the stability of the critical mode.

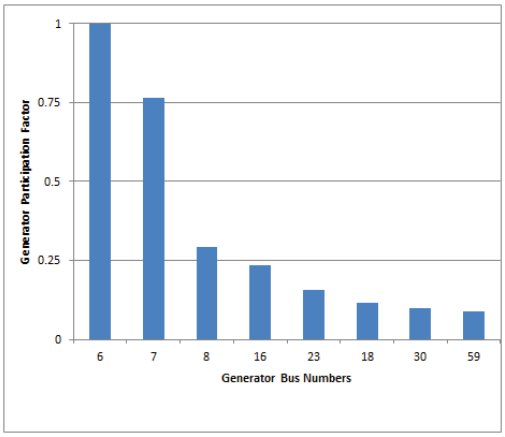

Fig. 5: The Largest Generator Participation factors

Table III shows the active and reactive power margins for the buses considered weak in the network.

TABLE III
ACTIVE AND REACTIVE POWER MARGINS FOR NETWORK WEAK BUSES

Bus No.	Voltage (p.u)	Active Power Margin (MW)	Reactive Power Margin (MVAr)
42	0.936	14.3099	2.9058

Nature Inspired Metaheuristic Optimization: A New Approach to Load Shedding

Charles Mwaniki[1]; Christopher Muriithi Maina[2]; Nicodemus Abungu[3]

[1]Electrical & Electronic Engineering Department, Thika Technical Training Institute,
P. O. Box 91-01000, Thika Kenya

[2]Electrical & Electronic Engineering Department, Jomo Kenyatta University of Agriculture and Technology,
P. O. Box 62000-00200, Nairobi Kenya

[3]Electrical & Electronic Engineering Department, University of Nairobi
P.O. Box 30197-00200, Nairobi, Kenya

e-mail:mwanikicharles2005@yahoo.com; cmmuriithi@eng.jkuat.ac.ke; abunguodero@uonbi.ac.ke

Abstract- Voltage stability has become a serious threat of modern power system operation nowadays. To tackle this problem properly, load shedding is one of the effective countermeasures. However, its consequences might result in huge technical and economic losses. Therefore, this control measure should be optimally and carefully carried out. Conventional methods of system load shedding are too slow and do not effectively calculate the correct amount of load to be shed. This results in either excessive or insufficient load reduction. Metaheuristic algorithms are becoming an important part of modern optimization. A wide range of Metaheuristic algorithms have emerged over the last two decades. This paper presents an overview of the extent to which metaheuristic algorithms have been utilized in optimal under frequency and under voltage load shedding**.**

Key-Words: - Cuckoo search, Metaheuristic optimization, Unconstrained optimization, Nature inspired algorithms

1. INTRODUCTION

Because of computational drawbacks of conventional numerical methods in solving complex optimization problems, researchers may have to rely on new algorithms. Heuristic algorithms typically intend to find a good solution to an optimization problem by 'trial-and-error' in a reasonable amount of computing time. Here 'heuristic' means to 'find' or 'search' by trials and errors. There is no guarantee to find the best or optimal solution, though it might be a better or improved solution than an educated guess. Any reasonably good solution, often suboptimal or near optimal, would be good enough for such problems. Broadly speaking, local search methods are heuristic methods because their parameter search is focused on the local variations, and the optimal or best solution can be well outside this local region. Metaheuristic algorithms are higher-level heuristic algorithms. Here, 'meta-' means 'higher-level' or 'beyond', so metaheuristic means literally to find the solution using higher-level techniques, though certain trial-and-error processes are still used. Broadly speaking, metaheuristics are considered as higher-level techniques or strategies which intend to combine lower-level techniques and tactics for exploration and exploitation of the huge space for parameter search [1-4].

There are two important components in modern metaheuristics, and they are: intensification and diversification, and such terminologies are derived from Tabu search . For an algorithm to be efficient and effective, it must be able to generate a diverse range of solutions including the potentially optimal solutions so as to explore the whole search space effectively, while it intensifies its search around the neibourhood of an optimal or nearly optimal solution. In order to do so, every part of the search space must be accessible though not necessarily visited during

the search. Diversification is often in the form of randomization with a random component attached to a deterministic component in order to explore the search space effectively and efficiently, while intensification is the exploitation of past solutions so as to select the potentially good solutions via elitism or use of memory or both [4-6].

Any successful metaheuristic algorithm requires a good balance of these two important, seemingly opposite, components [6]. If the intensification is too strong, only a fraction of local space might be visited, and there is a risk of being trapped in a local optimum, as it is often the case for the gradient-based search such as the classic Newton-Raphson method. If the diversification is too strong, the algorithm will converge too slowly with solutions jumping around some potentially optimal solutions. Typically, the solutions start with some randomly generated, or educated guess, solutions, and gradually reduce their diversification while increase their intensification at the same time, though how quick to do so is an important issue.

Another important feature of modern metaheuristics is that an algorithm is either trajectory-based or population-based. In trajectory-based algorithm, the path of the active search point (or agent) forms a Brownian motion-like trajectory with its movement towards some attractors. In population based algorithm, the parameter search is carried out by multiple agents in parallel. It is difficult to decide which type of method is more efficient as both types work almost equally successfully under appropriate conditions. A good combination of these two would lead to better metaheuristic algorithms.

2. NATURE INSPIRED METAHEURISTIC ALGORITHM

The naturally inspired metaheuristic algorithm includes genetic algorithms (GA), particle swarm optimization (PSO), simulated annealing (SA), ant colony optimization (ACO), bee algorithms (BA), harmony search (HS), firefly algorithms (FA), photosynthetic algorithm (PA), enzyme algorithm (EA) and Tabu search

3. APPLICATION OF METAHEURISTIC ALGORITHMS IN OPTIMAL LOAD SHEDDING.

In recent years, the word ‘metaheuristics’ refers to all modern higher-level algorithms [4], including Particle Swarm Optimization (PSO), Simulated Annealing (SA), Evolutionary Algorithms (EA) including Genetic Algorithms (GA), Tabu Search (TS), Ant Colony Optimization (ACO), Bee Algorithms (BA), Firefly Algorithms (FA), and, certainly Harmony Search (HS) and Cackoo search (CS)

Over the last decades, many meta-heuristic algorithms have been successfully applied to various engineering optimization problems. For most complicated real-world optimization problems, they have provided better solutions in comparison with conventional numerical methods. In regard to optimal load shedding the following nature inspired algorithm have been applied [1-4].

3.1 PARTICLE SWARM OPTIMIZATION

A new particle swarm optimization based corrective strategy to alleviate overloads of transmission lines is presented [6]. A direct acyclic graph (DAG) technique for selection of participating generators and buses with respect to a contingency is presented. Particle swarm optimization (PSO) technique has been employed for generator rescheduling and/or load shedding problem locally, to restore the system from abnormal to normal operating state. The effectiveness of the proposed approach is demonstrated for different contingency cases in IEEE 57 and modified IEEE 118 bus systems. The result shows that the proposed approach is computationally fast, reliable and efficient, in restoring the system to normal state after a contingency with minimal control actions.

Congestions or overloads in transmission network are alleviated by generation rescheduling and/or load shedding of participating generators and loads. The two

conflicting objectives 1) alleviation of overload and 2) minimization of cost of operation are optimized to provide pareto-optimal solutions. A multiobjective particle swarm optimization (MOPSO) method is used to solve this complex nonlinear optimization problem. A realistic frequency and voltage dependent load flow method which considers the voltage and frequency dependence of loads and generator regulation characteristics is used to solve this problem. The proposed algorithm is tested on IEEE 30-bus system, IEEE 118-bus system, and Northern Region Electricity Board, India (NREB) 390-bus system with smooth as well as nonsmooth cost functions due to valve point loading effect [7].

An optimal load shedding approach to enhance voltage stability employing a combination of modal analysis and particle swarm optimization (PSO) is presented[8],[19]. At first as a preventive control action the best transformers tap setting is indicated by PSO optimization to get the most possible voltage stability margin then as a corrective control action after contingencies the proposed approach is organized as a multi-objective optimization problem which reveals the best location and the lowest level of load shedding for special protection systems (SPS) in the direction of improving the voltage stability margin as well as the voltage profile.

A new optimization model to minimize power loss and the load curtailments necessary to restore the equilibrium of operating point is proposed [9]. The solution algorithm is based on the particle swarm optimization (PSO) method in which the load shedding would be considered as the penalty in the optimization cost function. The aim function would be optimized for minimum power loss under normal operating conditions and minimum load shedding during emergency conditions. In contrary to the other load shedding

A method for optimal allocation of fast and slow VAR devices using particle swarm optimization under different load levels is proposed [10]. These devices are supposed to be utilized to maintain system security in normal and contingency states, where corrective and preventive controls are implemented for the contingency cases. Load shedding and fast VAR devices are used in the corrective state in order to quickly restore system stability even they are expensive, while cheap slow VAR devices can be used in the preventive state to obtain the desired security level.

An approach to optimally allocate FACTS devices based on Expected Security Cost Optimal Power Flow (ESCOPF) under deregulated power system is proposed. The aims of the approach are both to minimize device investment cost and to maximize benefit defined as difference between Expected Security Cost (ESC) with and without FACTS installation. The problem is solved using Particle Swarm optimization (PSO) for attaining optimal FACTS allocation [11-13].

An automatic learning framework for the dynamic security control of a power system is presented. The proposed method employs a radial basis function neural network (RBFNN), which serves to assess the dynamic security status of the power system and to estimate the effect of a corrective control action applied in the event of a disturbance. Particle swarm optimization is applied to find the optimal control action, where the objective function to be optimized is provided by the RBFNN. The method is applied on a realistic model of the Hellenic Power System and on the IEEE 50-generator test system, and its added value is shown by comparing results with the ones obtained from the application of other machine learning methods [14].

3.2 GENETIC ALGORITHM

A new optimization approach for planning under-frequency load shedding using a variant of a genetic algorithm (GA) is described. The load shedding strategy consists of a given sequence of feeder disconnections, minimizing

total load curtailment while taking into account load dynamic characteristics [15-16].

A genetic algorithm (GA) is employed to search for the optimal supply restoration strategy in distribution networks. An 'integer permutation' encoding scheme is adopted in which each chromosome is a list of indices of switches. The status of each of these switches is decided according to graph theory subject to the radiality constraint of the distribution networks. Each chromosome then maps to a feasible network topology. A special gene '0' is also introduced into the chromosome. Instead of representing a switch, this is a flag that keeps some parts of the network disconnected enabling the GA to find the optimal load shedding strategy where necessary [17].

A novel planning method using genetic algorithm (GA) to achieve minimization of load shedding is proposed. The frequency of a power system declines rapidly when generator outage occurs. The general solution is to install sufficient under-frequency relays to pull frequency back to normal range. In this study, a single machine infinite bus (SMIB) is utilized to simulate system load with genetic algorithm for estimating the optimal load shedding and shedding ratio in each stage. Simulated results indicate that the proposed GA-based method is both feasible and effective to facilitate optimal load shedding planning [18].

3.3 ANT COLONY OPTIMIZATION

An ant colony optimization (ACO) based algorithm for solving the optimal load shedding problem is proposed. Two principal concerns of the problem are addressed. The appropriate load buses for the shedding are identified by sensitivities of voltage stability margin with respect to the load change at different buses. Then, the amount of load shedding at each bus is determined by applying ACO to solve a nonlinear optimization problem formulated in the optimal power flow framework. The performance of the proposed ACO based method is illustrated with a critical operating condition of the IEEE 30-bus test system [19].

4. DISCUSSION AND CONCLUSION

From the literature review described above it is evident that researchers have developed new optimization methods by imitating natural or behavioral phenomena on earth. The most commonly used metaheuristic being the particle swarm optimization. Genetic Algorithm and ant colony optimization have also been applied though not intensively. Although the HS algorithm has not been utilized at all in load shedding optimization, it has been successfully applied to a wide variety of practical optimization problems like pipe-network design [20], structural optimization [21], vehicle routing problem [22], combined heat and power economic dispatch problem [23], and scheduling of multiple dam system [24]. The Cuckoo search (CS) also has not been applied in optimization of load shedding. It is a newly evolved metaheuristic algorithm developed recently by Xin-She Yang and Suash Deb in 2009 [25]. It was proven in [18] that the CS was more generic and robust than the
PSO and GA in optimizing multimodal objective functions. Through simulations running on various standard test functions, CS was found to be more efficient in finding the global optima with higher success rates. This is partly due to the fact that there are fewer parameters to be fine-tuned in CS than in PSO and GA [26]. To the best of our knowledge, so far, CS was successfully used for mechanical engineering problems, which were spring design optimization and welded beam design [27]. Hence, CS has a great potential also to be as an effective alternative besides other evolutionary algorithms in handling load shedding optimization problems. There is therefore need for a research to be carried out to establish its feasibility in optimal load shedding.

5. REFERENCES

[1] Yang XS (2008) Mathematical Optimization: From Linear Programming

to Metaheuristics, Cambridge Int. Science Publishing, UK.

[2] Yang XS (2005) Biology-derived algorithms in engineering optimization. Handbook o]f Bioinspired Algorithms and Applications, Eds Olarius S and Zomaya A, Chapman & Hall/CRC

[3] Yang XS (2008) Nature-inspired Metaheuristic Algorithms. Luniver Press

[4] Glover F and Laguna M (1997) Tabu Search. Kluwer Academic Publishers

[5] Rad, B.F. ; Abedi, M. , "An optimal load-shedding scheme during contingency situations using meta-heuristics algorithms with application of AHP method", Optimization of Electrical and Electronic Equipment (OPTIM); 2008 , Page(s): 167 - 173

[6] Maharana, M.K., Swarup, K.S, "Particle Swarm Optimization based corrective strategy to alleviate overloads in power system" Nature & Biologically Inspired Computing, 2009. Pg 37 - 42

[7] Hazra, J. ; sinha, A. ,"Congestion management using multiobjective particle swarm optimization" Power and Energy Society General, 2008 IEEE , Pg: 1

[8] Jalilzadeh, S.; Hosseini, S.H.; Derafshian-Maram, M.,"Optimal load shedding to prevent voltage instability based on multi-objective optimization using modal analysis and PSO" Ultra Modern Telecommunications and Control Systems and Workshops (ICUMT), 2010 Page(s): 371 – 376

[9] He, Fei ; Wang, Yihong ; Ka Wing Chan ; Zhang, Yutong ; Shengwei Mei, "Optimal load shedding strategy based on particle swarm optimization" Advances in Power System Control, Operation and definition of optimal load shedding strategies" Electric Power Engineering, 1999

[17] Luan, W.P.; Irving, M.R.; Daniel, J.S., "Genetic algorithm for supply restoration and optimal load shedding in power system Management (APSCOM), 2009 , Page(s): 1 – 6

[10] Eghbal, M. ; El-Araby, E.E. ; Ito, Y. ; Zoka, Y. ; Yorino, N. , "A PSO Approach for VAR Planning Considering the Slow and Fast VAR Devices Prices", Systems, Man and Cybernetics(SMC), 2006, Page(s): 1849 - 1854

[11] Wibowo, R.S.; Yorino, N.; Zoka, Y.; Sasaki, Y.; Eghbal, M., "FACTS Allocation Based on Expected Security Cost by Means of Hybrid PSO" Power and Energy Engineering Conference (APPEEC), 2010, Page(s): 1 – 4

[12] Eghbal, M.; El-Araby, E.E.; Yorino, N.; Zoka, Y., "Application of metaheuristic methods to reactive power planning: a comparative study for GA, PSO and EPSO", Systems, Man and Cybernetics, 2007. Page(s): 3755 - 3760

[13] Eghbal, M. ; Yorino, N. ; El-Araby, E.E. ; Zoka, Y. , "Multi-load level reactive power planning considering slow and fast VAR devices by means of particle swarm optimisation" Generation, Transmission & Distribution, IET Volume: 2 , Issue: 5 ,2008 , pg 743 – 751

[14] Voumvoulakis, E.M.; Hatziargyriou, N.D., "A Particle Swarm Optimization Method for Power System Dynamic Security Control", Power Systems, IEEE Transactions Volume: 25 , Issue: 2 ; 2010 , Page(s): 1032 – 1041

[15] Mozafari, B.; Amraee, T.; Ranjbar, A.M., "An Approach for Under Voltage Load Shedding Using Particle Swarm Optimization ", Industrial Electronics, 2006 IEEE International Symposium ; 2006 , Page(s): 2019 – 2024

[16] Lopes, J.A.P.; Wong Chan Wa; Proenca, L.M. , "Genetic algorithms in the distribution networks" Generation, Transmission and Distribution, 2002, Page(s): 145 - 151

[18] Chao-Rong Chen ; Wen-Ta Tsai ; Hua-Yi Chen ; Ching-Ying Lee ; Chun-Ju Chen ; Hong-Wei Lan, "Optimal load shedding

planning with genetic algorithm", 2011 , Page(s): 1 - 6

[19] Nakawiro, W.; Erlich, I. "Optimal Load Shedding for Voltage Stability Enhancement by Ant Colony Optimization" Intelligent System Applications to Power Systems, 2009, Page(s): 1 - 6

[20] Z.W. Geem, J.H. Kim, and G.V. Loganathan, "Harmony search optimization: application to pipe network design", Int. J. Model. Simul, 22,(2), 125–133, 2002.

[21] K. S. Lee and Z.W. Geem, "A new structural optimization method based on the harmony search algorithm", Computers and Structures, 82, pp. 781–798, Elsevier, 2004.

[22] Z. W. Geem, K. S. Lee, and Y. Park, "Application of harmony search to vehicle routing", American Journal of Applied Sciences, 2(12), 1552-1557, 2005.

[23] A. Vasebi, M. Fesanghary, and S. M. T. Bathaeea, "Combined heat and power economic dispatch by harmony search algorithm", International Journal of Electrical Power and Energy Systems, Vol. 29, No. 10, 713-719, Elsevier, 2007.

[24] Z. W. Geem, "Optimal scheduling of multiple dam system using harmony search algorithm", Lecture Notes in Computer Science, Vol. 4507, 316-323, Springer, 2007.

[25] Cuckoo search. vol. 2011: Wikipedia, 2010.

[26] Yang, X.-S., Deb, S. Cuckoo Search via Lévy flights. In Proc.World Congr. on Nature & Biologically Inspired Computing (NaBIC 2009). India, 2009, p. 210-214.

[27] Yang, X.-S., Deb, S. Engineering optimization by cuckoo search. Int. J. Mathematical Modelling and Numerical Optimization, Dec 2010, vol. 1, no. 4, p. 330-343.

Analysis of Approximation Models of Power Coefficient Parameter in Variable Speed Wind Turbine Modeling

Ndirangu J.G[1], Nderu J.N[1], Muriithi C.M[1], Muhia A.M[2]
julzndirangu@gmail.com, adjainderuac@gmail.com,cmaina77@yahoo.com,ammuhia@gmail.com
[1]Department of Electrical and Electronic Engineering, Jomo Kenyatta University of Agriculture and Technology
[2]Department of Electrical and Electronic Engineering, Dedan Kimathi University of Technology

Abstract – Modeling a wind turbine is important in understanding its behavior especially for developing a controller for maximum power point tracking. The relationship between the various variables in a wind turbine and its output power constitutes the mathematical model of the wind turbine. Among these variables, the power coefficient is the most important especially for maximum power point tracking. It is a non linear function of tip speed ratio and blade pitch angle. This paper undertakes a survey of various numerical approximation models that have been proposed for the power coefficient parameter for given values of tip speed ratio and blade pitch angle. Maximum power point curves are then simulated using MATLAB and compared for the various models for a case study variable speed wind turbine. Simulation results and analysis show that one of the approximation models is the most appropriate for the case study wind turbine. This analysis will assist in development of a comprehensive control algorithm for maximum power point tracking for the variable speed wind turbine.

Keywords –wind turbine, power coefficient, maximum power point, tip speed ratio.

INTRODUCTION

Even though renewable energy is a good substitute for conventional sources, there is some skepticism associated with their performance and cost. Researchers have been working to address these concerns. A unique limitation of wind energy conversion systems is their inability to track peak power production efficiently at varying wind speeds. This has led to control algorithms referred to as Maximum power point (MPPT) algorithms[1].

MPPT involves optimizing the generator speed relative to the wind velocity intercepted by the wind turbine such that power extracted is maximized. MPPT methods can broadly be classified into those that use sensors and those that are sensorless. The sensorless methods track the maximum power point by monitoring the power variation [2], [3].

Methods that use sensors track maximum power point by control of rotor speed and torque to keep tip speed ratio at an optimal value. Tip speed ratio is the ratio of tip speed of rotor blades to the wind speed.

Sensorless MPPT methods have poor dynamic characteristics because they are not usually sensitive to variations in wind speed. Due to the non-negligible inertia of the wind turbine, the power output changes a bit lazily compared to change in wind speed, this challenge is overcome by the methods that use sensors since they directly measure the wind turbine speed and give the control reference instantaneously. However these methods require the characteristic of the wind turbine to be known.

Wind turbines may be variable pitch or fixed pitch meaning blades may or may not be able to rotate along their longitudinal axes [4]. For small wind turbines typically less than 10kW, the blade pitch is usually fixed to minimize design cost. They can also be variable or fixed speed. Variable speed wind energy systems have several advantages compared with fixed speed wind energy systems such as yielding maximum power output, developing low amount of mechanical stress, improving efficiency and power quality.

Maximizing power output from a wind turbine requires maximizing the power coefficient C_p for the varying wind speeds. Power coefficient is the ratio of the mechanical power at the turbine shaft to the power available in the wind, given as a function of tip speed ratio. To understand the behavior of C_p, numerical approximation models are used to simulate it for analysis. This paper carries out a comparison of several of these approximation models with the aim of

finding the appropriate one for a case study wind turbine.

According to [5],model validation involves defining the model and model structure to be used for modeling the device under study, collecting recorded or measured data from the actual device to be modeled, simulating the same events/ tests as occurred / forced during data collection using the model and then comparing the simulated results to recorded/ measured results.

WIND TURBINE MODELLING

Dynamic modeling and simulation is required to determine the effectiveness of a control strategy before deployment of a system.

The power extracted from the wind by a wind turbine rotor can be expressed as:

$$P_m = \frac{1}{2}\rho\pi R^2 v^3 C_p \quad (1)$$

Where

ρ = air density
R = radius of the rotor,
v = wind speed and
C_p = Power coefficient.

C_p represents the percentage of power available in the wind that is converted into mechanical power. It is a non linear function of the tip speed ratio λ as well as the blade pitch angle β i.e

$$C_p = C_p(\lambda, \beta) \quad (2)$$

Where

$\lambda = \frac{R\omega}{v}$ and

ω = rotation speed of the rotor.

The blade pitch angle is defined as the angle between the plane of rotation and the blade cross-section chord. As earlier stated, for small wind turbines, the blasé pitch angle is usually fixed.

A maximum for the function in equation (2) is known as Beltz limit. $C_{pmax} = 0.593$ [3]

This is the maximum possible turbine power coefficient. From equation (1) above, when controlling the wind turbine for power output maximization, C_p is useful as it is the only variable and controllable parameter. Wind speed v is a variable but not controllable.

There is a value of λ for which C_p is maximum, therefore yielding maximum power for a given wind speed v.

Because of the relationship between C_p and λ for each wind velocity, there is a turbine speed that gives maximum output power.

Modelling is essential in developing a controller for maximum power point tracking.

Various authors have proposed different numerical approximation models for the power coefficient parameter Cp for given values of λ and β . For a fixed pitch wind turbine as is the case with our case study wind turbine, β is set to a constant value.

The author in [6] proposes the model given by:

$$C_p = \frac{1}{2}\left(\frac{116}{\lambda_i} - 0.5\beta - 5\right)e^{-21/\lambda_i} \quad (3)$$

where

$$\lambda_i = \frac{1}{\frac{1}{\lambda + 0.089\beta} - \frac{0.035}{\beta^3 + 1}}$$

Similarly, the author in [7] used the model defined by:

$$C_p = 0.22\left(\frac{116}{\lambda_i} - 0.4\beta - 5\right)e^{-12.5/\lambda_i} \quad (4)$$

where:

$$\lambda_i = \frac{1}{\frac{1}{\lambda - 0.02\beta} - \frac{0.003}{\beta^3 + 1}}$$

According to the authors in [8] the $C_p(\lambda)$ curve of the wind turbine can be expressed approximately using the following polynomial:

$$C_p(\lambda) = a_1 + a_2\lambda + a_3\lambda^2 + a_4\lambda^3 + a_5\lambda^4 + a_6\lambda^5 \quad (5)$$

Through adjusting the coefficients a1-a6 in the above polynomial equation (5), the

shape of the $C_p(\lambda)$ curve can be modified.

For the case study wind turbine the appropriate coefficients are found to be:

$a_1 = 0.04, \quad a_2 = 0.133, \quad a_3 = 0.146,$
$a_4 = 0.602 \; a_5 = 0.104 \; a_6 = 0.0006$

SIMULATION RESULTS AND ANALYSIS

The specifications parameters for the case study commercial wind turbine are given in Table 1.

The parameters shown in Table1 were defined and the operating parameters set in MATLAB program code.

The three numerical approximation models described by equations (3) to (5) were then simulated using MATLAB.

The plots of interest are those on the maximum power point curves for various wind speeds.

Case study wind turbine	Rhino Rotor Wind Turbine
Manufacturer	PowerGen East Africa Ltd.
Rated Power	1Kw at 12.5m/s
Rotor Diameter	3.1m
Startup wind speed	3.2m/s
Over speed protection	Mechanical tail furling

Table1: Parameters of case study wind turbine

The plots for maximum power point curves and Cp vs λ are as shown in figures 1 to 4 below.

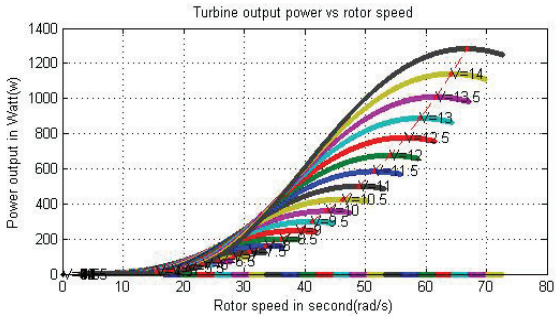

Fig.1: Power output vs rotor speed using approximation model in equation (3)

From the plot of Fig. 1 it can be seen that the power output at the rated speed of 12.5 m/s is 777.5W

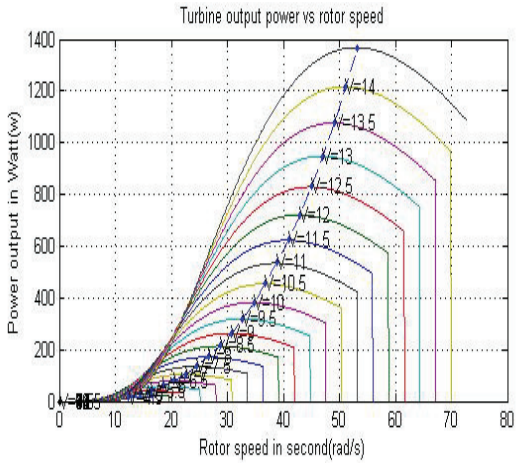

Fig.2 Power output vs rotor speed using approximation model in equation (4)

From the plot of Fig. 2 it can be seen that the power output at the rated speed of 12.5 m/s is 829.1W

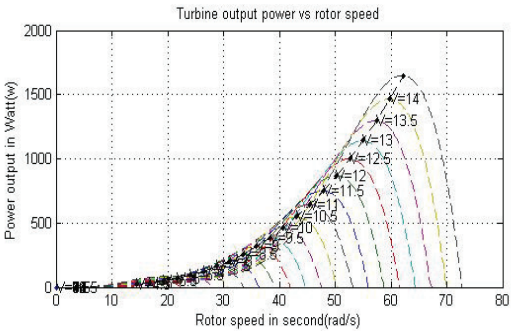

Fig.3 Power output vs rotor speed using approximation model in equation (5)

From the plot of Fig. 3 it can be seen that the power output at the rated speed of 12.5 m/s is 999.6W

Fig.4 shows power output vs rotor speed for all the 3 approximation models on the same scale.

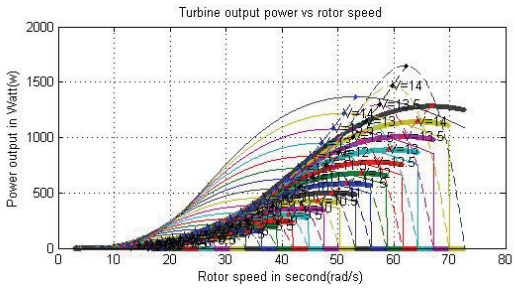

Fig.4. Power output vs rotor speed for all the 3 approximation models

Fig.4 shows that the three models are comparable for the case study wind turbine although giving different maximum power values.
From the results it can be seen that the different models give different values of maximum power points for the same wind speed.
To validate their accuracy, the maximum power point at the rated wind speed (12.5m/s) for the case study wind turbine as given by the various models was compared to the actual value from the manufacturer's datasheet.

The results are as shown in Table 2:

Model	Maximum power at 12.5m/s wind speed(W)	%Accuracy
1	777.5	77.75%
2	829.1	82.91%
3	999.5	99.95%

Table 2: Comparison of maximum power points at rated wind speed for the three models.

From the manufacturer's datasheet of the case study wind turbine, the power output at the rated wind speed is 1000W.
It can be seen that at rated wind speed, approximation model in equation (3) has 77.77% accuracy in predicting the power output. Approximation model in equation (4) has 82.91% accuracy while that in equation (5) has 99.95% accuracy.

A plot of Power coefficient C_p vs Tip speed ratio λ for the three models was also obtained as in figure 5.

Fig.5 $C_p$vs λ for all the 3 approximation models.

The figure shows the maximum power coefficients of the three models. Approximation model in equation(1) gives maximum value of Cp as 0.1605, model in equation (4) as 0.1712 and that in equation (5) as 0.2063. It can be seen that model in equation (5) gives the highest value of Cp at 0.2063

CONCLUSION
For maximum power point tracking it is important to use a model that gives the maximum power for various wind speeds.
From the analysis, it can be seen that approximation model described by equation (5) is the one that best approximates power coefficient C_p for the case study wind turbine as well as giving highest power for all wind speeds as compared to the other models. It gives has an accuracy of 99.95% in giving power output at the rated wind speed.
It also gives the highest value of maximum C_p at 0.2063, hence giving maximum power output for the case study wind turbine.
This model will be used to develop a controller for maximum power point tracking for the case study wind turbine.

REFERENCES

[1] Shrikant S Mali1, B. E. Kushare, "MPPT Algorithms: Extracting Maximum Power from Wind Turbines," *International Journal of Innovative Research In Electrical, Electronics, Instrumentation and Control Engineering,* Vol. 1, Issue 5, August **2013**

[2] Xing –Peng et al, "A Fuzzy logical MPPT control strategy for PMSG wind generation systems", *Journal of Electronic Science and Technology*, Vol 11, No.1, March **2013**

[3] Kazmi S.M.R. et al, " A novel algorithm for fast and efficient speed-sensor less maximum power point tracking in wind energy conversion systems", *IEEE Transactions on Industrial Electronics.*. **2011**,

[4] Kathryn E. Johnson and Lucy Y. Pao, "A tutorial on the dynamics and control of wind turbines and wind farms", *Proc. American Control Conference*, **2009**.

[5] Mohamed Asmine et al, "Model validation for wind turbine generator models", *IEEE Transactions on Power systems*, **2010**

[6] R. Jagatheesan, K. Manikandan, "An Efficient Variable Speed Stand Alone Wind Energy Conversion System & Efficient Control Techniques for Variable Wind Applications", *International Journal of Advances in Engineering & Technology*, Nov. **2012**

[7] T. F. Chan and L. L. Lai, "Permanent-magnet machines for distributed generation: A review," in *Proc. IEEE Power Eng. Annu. Meeting*, **2007**.

[8]Bogdan S. Borowy and Ziyad M. Salameh,"Dynamic Response of a Stand-Alone Wind Energy Conversion System with Battery Energy Storage to a Wind Gust", *IEEE Transactions on Energy Conversion*, Vol. 12, No. 1, March **1997**.

OPTIMAL LOCATION OF SVC FOR MINIMIZING THE COST OF GENERATION

IRENE MUISYO, C. M. MAINA, ROY ORENGE

muisyoirene@gmail.com, cmaina77@yahoo.com, samroyoin@gmail.com

EEE SEEIE JKUAT, EEE SEEIE JKUAT, EEE DeKUT

P.O. Box 62000 – 00200, Juja, Nairobi, Kenya.

Abstract - Flexible AC Transmission System (FACTS) devices in power systems play a vital role in the power system performance, such as improving system stability, increasing system loading capability, reducing losses and the cost of generation. In order to maximize their benefits, these devices must be located optimally. In this paper, optimal location of SVC is obtained by use of two benefit factors which are obtained and weighted by Analytical Hierarchy Process (AHP). Placement of SVC is then done at the obtained location and Optimal Power Flow (OPF), voltage analysis and an estimation of the cost of investment recovery are performed. This proposed method is tested on WSCC 9-bus and modified IEEE 30-bus test systems. Results obtained show an improved voltage profile and minimization of generation cost.

Keywords: VAR compensation, FACTS devices, SVC, voltage profile.

I. INTRODUCTION

Transmission of reactive power results to increased losses in the transmission system, decrease in the real power transmitted, and changes in the voltage amplitude at the end of the line. It is therefore necessary to provide reactive power compensation, at the right location in the power system, in order to increase transmitted power, decrease losses and provide stability of voltage amplitude at the end of the line (Tosun, 2012).

Traditionally, the locations for placing new VAR sources were either simply estimated or directly assumed (Wenjuan Zhang, 2007). With the deregulation of the electricity market, the traditional concepts and practices of power systems are changing. FACTS devices such as Static VAR Compensator (SVC), Thyristor Controlled Series Compensation (TCSC) and Unified Power Flow Controller (UPFC) are being adopted in many countries.

FACTS devices are power electronic based devices which can change transmission system parameters like impedance, voltage and phase angle. This allows control of power flow in the network, reduction of flows in heavily loaded lines, lower system losses, improved stability of network and reduced cost of production. It is important to ascertain the location of these devices because of their significant costs (S. B. Bhaladhare, 2012) (Rakhmad Syafutra Lubis, 2012).

Optimal VAR location of different devices has been attempted using various techniques over the last few years. (N.M. Tabatabaei, 2011) presents PSO and APSO-SA methods for ascertaining optimal location of FACTS devices to achieve minimum VAR cost while satisfying the power system constraints, for single and multi-type FACTS devices. (S. B. Bhaladhare, 2012) discusses optimal placement of FACTS devices based on Voltage Stability Index (VSI) to obtain their location and operating parameters for improving voltage profile in a power system.

Location and type of various FACTS controllers has also been investigated in (Rakhmad Syafutra Lubis, 2012) using the sensitivity of system loading factor method and solved with the nonlinear predictor-corrector primal-dual interior-point optimal power flow (OPF) algorithm. Performance evaluation of Newton-Raphson power flow analysis method has been done on IEEE-30 bus system in (Amit Debnath, 2013) to investigate effect of UPFC on the voltage profile.

This paper seeks to obtain the optimal location of SVC by use of a real power loss minimization algorithm. Benefit factors are evaluated from the results and weighted by use of AHP. OPF is then done with SVC incorporation. Lastly, voltage analysis and comparison of savings made from their utilization will be done to determine if it is economical to invest in FACTS devices.

This paper is organized as follows: section II presents SVC modelling and its optimal location, while problem formulation and case study are in section III. Simulation results and discussion are found in section IV and conclusion section V.

II. FACTS DEVICES

FACTS devices can regulate the active and reactive-power flow as well as system voltage magnitude simultaneously by their fast control characteristics and their continuous compensating capability. Series compensation modifies line reactance X_{ij} while shunt compensation injects reactive power which improves the voltage (Rakhmad Syafutra Lubis, 2012) (J.Vivekananthan, 2013).

Static VAR Compensator (SVC)

SVCs regulate voltages at its terminals by controlling the amount of reactive power injected into or absorbed from the power system. If the power systems reactive load is capacitive (leading), the SVC will use reactors to consume VARs from the system, lowering the system voltage. Under inductive (lagging) conditions, the capacitor banks are automatically switched in, thus providing a higher system voltage (D. Murali, 2010). The model is incorporated into the sending end as a shunt element of the transmission line as shown in Fig. 1.

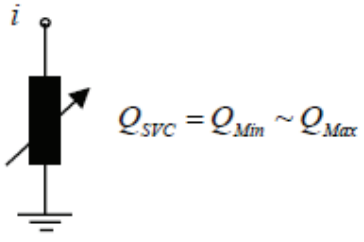

Fig 1: Power Injection Model of SVC

OPTIMAL LOCATION OF SVC

Due to the high cost of FACTS devices, it is necessary to locate them properly in order to maximize their benefits. Two benefit factors evaluated in this paper are:

a) Voltage Benefit Factor (VBF)

$$VBF_i = \sum_{i \in n} \frac{(V_i(Q_{si}) - V_{io})}{Q_{si}} \; x \; 100\% \; i \qquad (1)$$

where $V_i(Q_{si})$ and V_{io} is the voltage magnitude at load bus i, with and without VAR compensation respectively and Q_{si} is the amount of VAR support in the bus. n is the number of load buses.

b) Loss Benefit Factor (LBF)

$$LBF_i = \sum_{i \in n} \frac{(P_{Lo} - P_L(Q_{si}))}{Q_{si}} \; x \; 100\% \; i \qquad (2)$$

where $P_L(Q_{si})$ and P_{Lo} is the power transmission loss in the system with and without VAR compensation respectively (Zhu, 2009) (Jigar S.Sarda, 2012) (J.Vivekananthan, 2013).

Analytic Hierarchy Process (AHP)

The AHP is a decision making approach which presents an objective function, criterion and alternatives. It evaluates trade-offs and performs a synthesis to arrive at a final decision (Saaty, 2008). In this paper, the AHP technique is applied with the objective of identifying the optimal location of SVC. The criterion is VBF and LBF, while alternatives are the various load buses which are candidate sites for VAR support. The judgement matrix to be used (Zhu, 2009) is presented below:

	VBF_i	LBF_i
VBF_i	1	½
LBF_i	2	1

The weighting coefficients of the judgment matrix are computed through the sum method as

$$W = [0.667, 0.333]$$

III. PROBLEM FORMULATION

This is done in two stages:

a) Optimal location of SVC

Optimal location of SVC can be done using various objective functions as detailed in (Wenjuan Zhang, 2007). The approach taken in this paper is minimizing real power loss of the system while observing all system constraints. Mathematically, it is expressed as:

$$F = \min(P_{loss}) = \min\left(\sum_{i=1}^{NL} g_{i,j}\left(V_i^2 + V_j^2 - 2V_iV_j\cos(\delta_i - \delta_j)\right)\right) \quad (3)$$

where V_i is voltage magnitude at bus i; $g_{i,j}$ is conductance of line $i-j$; δ_i is voltage angle at bus i and NL is the total number of transmission lines in the system.

SVC constraint:

$$Q_{SCV,min} \leq Q_{SCV} \leq Q_{SCV,max} \quad (4)$$

where Q_{SCV} is the reactive power injected into the bus by SVC.

b) Generation cost minimization with SVC incorporated

This is the conventional OPF whose objective function is:

$$F = min\left(F(P_G)\right) = \sum_{i=1}^{NG} a_iP_{Gi}^2 + b_iP_{Gi} + C_i \quad (5)$$

Both objectives are subject to:

Power balance (equality) constraints: The total power generated by the units must be equal to the sum of total load demand and total real power loss in the transmission lines.

$$P_G - P_D - \sum_{j\in N} |V_i||V_j||Y_{ij}|\cos(\theta_{ij} + \delta_j - \delta_i) = 0 \quad (6)$$

$$Q_G - Q_D - \sum_{j\in N} |V_i||V_j||Y_{ij}|\sin(\theta_{ij} + \delta_j - \delta_i) = 0 \quad (7)$$

where P_G is the total active power generated and P_D is the total active power demand of the system. Q_G is the reactive power generated and Q_D is the reactive power demand of the system.

Inequality constraints

Power generating limits: each generator in operation has a minimum and maximum permissible output.

$$P_{Gi,min} \leq P_{Gi} \leq P_{Gi,max} \quad (8)$$

$$Q_{Gi,min} \leq Q_{Gi} \leq Q_{Gi,max} \quad (9)$$

Transmission line limits: this is the maximum power a given transmission line is capable of transmitting.

$$S_{ij} \leq S_{ij\ max} \quad i \neq j \quad (10)$$

Voltage limits: imposed for bus voltage magnitudes in order to maintain the voltage profile.

$$V_{i,min} \leq V_i \leq V_{i,max} \quad (11)$$

(D P Kothari, 2003)

Capital cost of SVC

The capital cost of SVC is given as:

$$C_{SVC} = 0.0003S^2 - 0.3051S + 127.38\ (US\$/kVAr) \quad (12)$$

where S is the operating range of device obtained as: $S = |Q_2| - |Q_1|$

Q_2 is the reactive power in the system after installing FACTS devices and Q_1 is the reactive power in the system before installing FACTS devices (N.M. Tabatabaei, 2011) (Kalaivani R., 2012).

CASE STUDY

Optimizing process and placement of SVC has been tested on two systems: Western System Coordinating Council (WSCC) 9-bus and modified IEEE 30-bus system. WSCC 9-bus test system has 3 generators on bus 1, 2 and 3 (S. B. Bhaladhare, 2012). Modified IEEE 30-bus system has 6 generators on bus 1, 2, 5, 8, 11, and 13 (Zhu, 2009). Generator data is found on the appendix. MATPOWER (v2), a toolbox of MATLAB, has been used for simulations.

IV. SIMULATION RESULTS

Case 1: Optimal location of SVC

SVC is placed at all load buses. LBFs and VBFs are calculated, then AHP used to determine the best location for SVC. The bus with the highest weight coefficient signifies the largest system benefit in terms of voltage, loss and cost of generation. Figure 2 shows the proposed VAR support sites and the corresponding weighting coefficients for the 9-bus system.

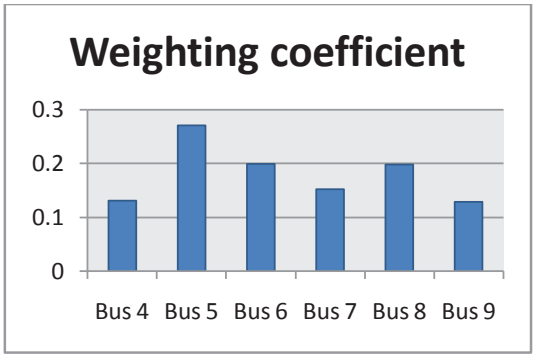

Fig 2: WSCC 9-bus test system

The top three sites in the WSCC 9-bus system for placing VAR compensation is bus 5, 8, and 6. Bus 5 has the highest weighting coefficient hence the optimal location of SVC.

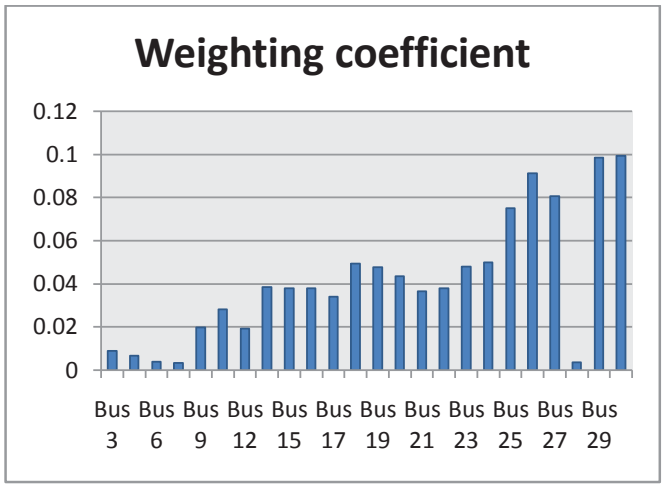

Fig 3: Modified IEEE 30-bus system

The top three sites in the IEEE 30 - bus system for placing VAR compensation is bus 30, 29 and 26, with the optimal location being bus 30.

Case 2: Voltage analysis

Plot of voltage magnitude for both systems, without and with SVC are shown in fig 4 and 5.

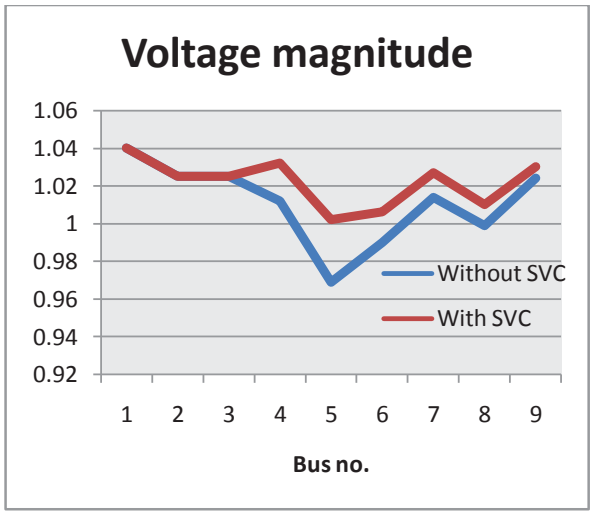

Fig 4: WSCC 9-bus system

The voltage profile has improved. Bus 5 had the lowest voltage magnitude of 0.969p.u., which rose to 1.002p.u. after SVC incorporation.

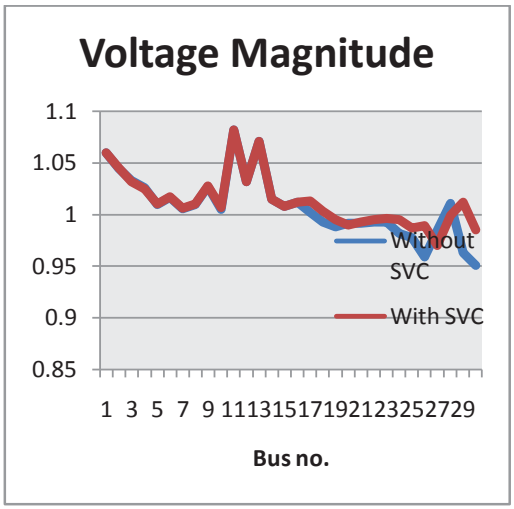

Fig 5: IEEE 30-bus system

Bus 30 had the lowest voltage of 0.951p.u., which rose to 0.985 p.u. after SVC incorporation.

POWER SYSTEM LOSS

The real and reactive total system losses for both systems are found in table 1 and 2 below, with and without SVC.

Table 1: WSCC 9 bus-system

	Without SVC	With SVC
Real power loss (MW)	7.437	6.86
Reactive power loss (MVAR)	77.63	71.63

Total system losses reduced with SVC incorporation for WSCC 9-bus system.

Table 2: Modified IEEE 30-bus system

	Without SVC	With SVC
Real power loss (MW)	9.251	9.569
Reactive power loss (MVAR)	39.2	40.02

From table 2, real and reactive power losses slightly increased with SVC incorporation. This is due to change in dispatch, whereby the cheapest generating unit increases real power production, resulting in higher power flows, hence losses in some lines.

The total cost of generation in both systems is however reduced and savings are used as signals for capital cost recovery, below.

Investment cost recovery

Table 3: WSCC 9-bus system

Cost of generation ($/hr)	
Without SVC	7805.95
With SVC	7754
Savings	51.95

Operating range is evaluated as $18MVAR$ and capital cost of SVC $US\$91{,}835.58$. With a utilization factor of 40%, payback period is 0.51 years.

Table 4: modified IEEE 30-bus system

Cost of generation ($/hr)	
Without SVC	883.74
With SVC	865.56
Savings	18.18

Operating range is evaluated as $8MVAR$ and capital cost of SVC $US\$16{,}886.58$. With a utilization factor of 40%, payback period is 0.26 years.

V. CONCLUSION

In this paper, a method for optimal placement of SVC has been proposed for reducing the cost of generation in a power system. The proposed method is tested on the WSCC 9-bus and modified IEEE 30-bus test systems and results obtained show that SVC placement on the appropriate bus results in a great reduction in cost of generation and improves the voltage profile.

Appendix

WSCC 9-BUS SYSTEM

Table A1 & A2: Generator Data

Bus. no.	Generator limits			
	Pmax	**Pmin**	**Qmax**	**Qmin**
1	250	10	300	-300
2	300	10	300	-300
3	270	10	300	-300

Bus. no.	Generator cost coefficients		
	a	**b**	**c**
1	0.150	5.0	150
2	0.085	1.2	600
3	0.123	1.0	335

MODIFIED IEEE 30-BUS SYSTEM

Table A3 & A4: Generator Data

Bus. no.	Generator limits			
	Pmax	**Pmin**	**Qmax**	**Qmin**
1	200	50	250	-20
2	80	20	100	-20
5	50	15	80	-15
8	35	10	60	-15
11	30	10	50	-10
13	40	12	60	-15

Bus. no.	Generator cost coefficients		
	a	**b**	**c**
1	0.020	2.00	0
2	0.018	1.75	0
5	0.063	1.00	0
8	0.008	3.25	0
11	0.025	3.00	0
13	0.025	3.00	0

References

Amit Debnath, C. N. (2013). Voltage Profile Analysis for IEEE 30 Bus System Incorporating with UPFC. *International Journal of Engineering and Advanced Technology* , 763-769.

D P Kothari, I. J. (2003). *Modern Power System Analysis.* New Delhi: Tata MCGraw Hill.

D. Murali, M. R. (2010). Comparison of FACTS Devices for Power System Stability Enhancement. *International Journal of Computer Applications* , 30-36.

J.Vivekananthan, R. (2013). VOLTAGE STABILITY IMPROVEMENT AND REDUCE POWER SYSTEM LOSSES BY BACTERIAL FORAGING OPTIMIZATION BASED LOCATION OF FACTS DEVICES. *International Electrical Engineering Journal* , 1034-1040.

Jigar S.Sarda, V. N. (2012). Genetic Algorithm Approach for Optimal location of FACTS devices to improve system loadability and minimization of losses. *International Journal of Advanced Research in Electrical, Electronics and Instrumentation Engineering* , 114-126.

Kalaivani R., V. K. (2012). Enhancement of Voltage Stability by Optimal Location of Static Var Compensator Using Genetic Algorithm and Particle Swarm Optimization. *American Journal of Engineering and Applied Sciences* , 70-77.

N.M. Tabatabaei, G. A. (2011). OPTIMAL LOCATION OF FACTS DEVICES USING ADAPTIVE PARTICLE SWARM OPTIMIZATION MIXED WITH SIMULATED ANNEALING. *International Journal on Technical and Physical Problems of Engineering* , 60-70.

Rakhmad Syafutra Lubis, S. P. (2012). Selection of Suitable Location of the FACTS Devices for Optimal Power Flow. *International Journal of Electrical & Computer Sciences* , 38-50.

S. B. Bhaladhare, P. B. (2012). Enhancement of Voltage Stability through Optimal Location of SVC. *International Journal of Electronics and Computer Science Engineering* , 671-678.

Saaty, T. L. (2008). Decision making with the analytic hierarchy process. *Internaional Journal Services Sciences* , 83-99.

Tosun, S. (2012). Investigation of controller effects of SVC and STATCOM on power systems. *Energy Education Science and Technology* , 749-760.

Wenjuan Zhang, F. L. (2007). Review of Reactive Power Planning: Objectives, Constraints, and Algorithms. *IEEE TRANSACTIONS ON POWER SYSTEMS* , 2177-2187.

Zhu, J. (2009). *OPTIMIZATION OF POWER SYSTEM OPERATION*. New Jersey: John Wiley & Sons, Inc.

Dynamic Voltage Stability Analysis of the Kenya Power System using VCPI Stability Index and Artificial Neural Networks

[1]Njoroge S. N, [2]Muriithi C. M, [3]Ngoo L. M

[1,2]JomoKenyattaUniversity of Agriculture & Technology

Department of Electrical & Electronic Engineering

snnjoroge@jkuat.ac.ke

[3]Multimedia University

***Abstract* - Dynamic voltage stability deals with the voltage levels and how they are affected by either faults or load changes within the system.Voltage instability has long been suspected in the voltage collapse and islanding of power systems. Identifications of operational conditions leading to voltage collapse is therefore critical in allowing for critical defensive measures by the system operator to avoid voltage collapse before it occurs. This paper examines the use of Voltage Collapse Proximity Indicator (VCPI) in conjunction with Artificial Neural Networks to predict conditions of voltage instability before they occur for load buses within the Kenya power system that can be used for online prediction of voltage stability within the system.**

Keywords – Voltage Stability, VCPI, ANN

I. INTRODUCTION

Voltage stability is the ability of a power system to maintain voltage magnitudes at all system buses within a specified margin both under normal operating conditions and after being subjected to a disturbance. Voltage instability has long been suspected in system wide blackouts. As a result, voltage stability has been studied in depth both for static and dynamic voltage stability. Static voltage stability is concerned with the system when operating under given loading and generation conditions while dynamic stability is concerned with the changes in the system when it undergoes significant load changes or contingencies in lines or generators. To evaluate how voltage stable a bus is, the Voltage Collapse Proximity Indicator (VCPI) is one of the tools employed recently.It incorporates elements of the Y-bus matrix to capture the network topology as well as the real and reactive power configurations both at the reference bus and within the system as a whole. The VCPI can however only be calculated for static conditions and in this paper minute load changes are used to simulate dynamic loading and contingency conditions.

Artificial intelligence techniques have also been used for a while to reduce the computation times in the power flow solution which is an iterative procedure. Artificial Neural Networks (ANN) are used to mimic human brain cognitive properties and can be trained to read patterns in related data that may be too complex to capture in mathematical terms. In this paper, ANNs are trained using data from the load flow simulations and the corresponding VCPI indices to give predictions of the corresponding voltage magnitudes to expect at each bus.

II. METHODOLOGY

A. POWER FLOW PROBLEM

The power flow solution is used to determine the voltage magnitude and angle at each bus within the system as well as the real and reactive power flows and losses along all lines within the system for a given configuration of loads and generation. Using the nodal current equations, the current entering the i^{th} bus of an n-bus system can be obtained by

$$I_i = V_i \sum_{j=0}^{n} Y_{ij} - \sum_{j=1}^{n} Y_{ij} V_j \qquad (1)$$

At bus I, the power injected is given by

$$\frac{P_i - jQ_i}{V_i^*} = I_i \qquad (2)$$

Equating the 2 equations gives

$$\frac{P_i - jQ_i}{V_i^*} = V_i \sum_{j=0}^{n} Y_{ij} - \sum_{j=1}^{n} Y_{ij} V_j \qquad (3)$$

Equation (3) is a system of algebraic non-linear equations that is solved by iterative techniques. The

most popular is the Newton-Raphson method which gives fast convergence on a solution due to its quadratic convergence.The powerflow equations (1) and (2) are solved to give

$$\begin{bmatrix} \Delta\delta \\ \Delta|V| \end{bmatrix} = \begin{bmatrix} J_1 & J_2 \\ J_3 & J_4 \end{bmatrix}^{-1} \begin{bmatrix} \Delta P \\ \Delta Q \end{bmatrix} (4)$$

J is the Jacobian matrix while the left hand side gives the correction vector that updates earlier values of δ and ***V***. In this paper, the Newton Raphson is run for a maximum of 100 iterations to obtain a single solution convergence.

B. VOLTAGE STABILITY

A power system at a given operating state and subject to a given disturbance is ***voltage stable***if voltages near loads approach post-disturbance equilibrium values[2]. Voltages of the buses within a power system are required to remain within 4% or 5% of the nominal bus voltage in line with ANSI standard C84.1. Voltage Stability can broadly be classified into Static Voltage Stability and Dynamic Voltage Stability.

Static Voltage Stability evaluates the voltage magnitudes at all the buses in the system for a given loading and system configuration. The result only applies to that network topology and loading condition. Dynamic Voltage Stability is concerned with 2 aspects of voltage stability [1]

i. Distance to instability – this measures how close the system is to being voltage unstable. The distance is given in terms of system parameters like loading, power flow across a critical line or reactive power reserve.
ii. Mechanism of Voltage Instability – this investigates what system factors contribute to voltage instability and what indicates that the system is heading towards instability.

Previous studies on Dynamic Voltage Stability have used singular value decomposition, multi-variable control theory and bifurcation analysis[3-7]. Since voltage stability is affected by slow acting system dynamics which allows for the use of many static points to analyse Dynamic Voltage Stability. In this paper, the static points are evaluated by continuously varying loads at a high resolution of 0.001pu and carrying out power flow solutions at each loading configuration.

C. VOLTAGE COLLAPSE PROXIMITY INDICATOR (VCPI)

The VCPI is a relatively new indicator gaining popularity for Voltage Stability Studies. It can be calculated at each bus for each loading and contingency condition [8]. It is calculated at bus *j* as

$$L_j = \left| \frac{S_{j+}^*}{Y_{jj+} V_j^2} \right| \quad (5)$$

Where

$$S_{j+} = S_j + S_{jcorr} \quad (6)$$

$$S_{jcorr} = \left\{ \sum_{\substack{i \in Loads \\ i \neq j}} \frac{Z_{ji}^*}{Z_{jj}^*} \frac{S_i}{V_i} \right\} V_j \quad (7)$$

And

$$Y_{jj} = \frac{1}{Z_{jj}} \quad (8)$$

$S_{jcorr}$is a component of all the other loads in the system incorporated into the index at bus *j*. The VCPI is calculated for the load buses within the system. It has a value of 0 for stability and 1 for complete instability

D. ARTIFICIAL NEURAL NETWORKS (ANN)

These have previously been used for identifying weak buses within a system [9]. They are used to model complex relationships that are difficult to model with mathematical equations or for which relationships exist but are unknown. They mimic the human brain.An extremely important and human characteristic of ANN is their adaptive nature, where learning by experience replaces programming in solving problems. ANNs learn the pattern on which they are trained. An artificial neuron consist of synapses which apply weights to the inputs, an adder***(+)*** that sums the weighted inputs and an activation function ***g(v)*** that maps the sum to the output function of the neuron as shown in Fig. 1. ANNs are formed by arranging neurons in layers. The input layer has input neurons where each input into the network feeds into each of the neurons in the input layer. The input layer's output is fed into the middle layer containing several neurons. The middle layer's output is then fed into the output layer which normally has a single neuron with a single output. Varying the

number of neurons in the middle layer affects the accuracy of the whole ANN.

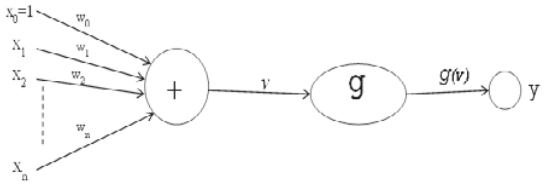

Fig.1: Artificial Neural Network

III. RESULTS

The 9-bus WSCC system was used to test the accuracy of the VCPI calculations using static load increments. The loading on Bus 5 was increased in steps of 0.001pu while maintaining pf until when the power flow solution did not converge. This occurred at 2.971pu loading and the corresponding plot of the VCPI and voltage magnitude was as in Fig 2.

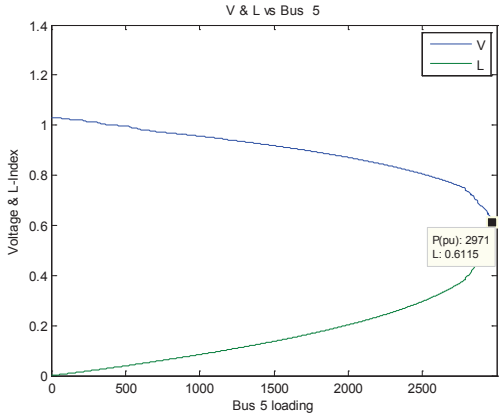

Fig.2 : Bus 5 V & L (WSCC 9-bus system)

This result matched previous studies using the VCPI [10] with the collapse point for Bus 5 occurring at 2.971pu (371+j149MVA).

Next the IEEE 14-bus system was studied. This involved iterations for the ideal case and with *n-1* contingency. The contingencies were selected as line contingences and for transformers the tap settings were varied between 90% and 110% of the nominal tap setting. At each iteration, 100 random loading configurations of between 30% and 200% at each load bus without maintaining pf. Within each of these iterations, a load flow study was run with the single contingency and load configuration. From the load flow, the voltage magnitudes, real and reactive power at each bus and for the whole system were recorded. Also, the L-index was calculated for that configuration. This data was then used to train an ANN with 100 neurons in the hidden layer. Previous studies [11] found bus 14 is the weakest bus in the system. A comparison of the VCPI calculated from the Power Flow and that predicted by the ANN is shown in Table 2

All Values in pu				n-1		
P_{14}	Q_{14}	P_{tot}	Q_{tot}		Method	VCPI
1	1	1	1	0	**Calculated**	0.0279
					ANN	0.0259
0.98	0.71	0.91	0.90	2	**Calculated**	0.0303
					ANN	0.0277
1.15	1.45	0.99	1.11	10	**Calculated**	0.0394
					ANN	0.0263
0.55	0.8	1.04	0.87	18	**Calculated**	0.0466
					ANN	0.0449
1.31	1.44	1.07	1.16	18	**Calculated**	0.0207
					ANN	0.0090

Table 1: VCPI for IEEE 14 bus System

From Table 1, it is clear that as the total system load increases, the VCPI value increases. Similarly, increased loading on bus 14 increases the VCPI value, indicating increased instability. The ANN values also follow the power flow calculated values. Since the VCPI varies from 0-1, the relative error is very minimal.

The same algorithm was then used on the 37-bus Kenyan system. Previous studies [12] identified buses 10,22,30,31 as the weakest buses in the system. The VCPI for the 3 buses using power flow and ANNs are shown in tables 2, 3 and 4.

All Values in pu				n-1		
P_{10}	Q_{10}	P_{tot}	Q_{tot}		Method	VCPI
1	1	1	1	0	**Calculated**	0.007928
					ANN	0.007935
1.04	1.50	0.86	1.08	20	**Calculated**	0.008729
					ANN	0.008658
1.40	1.15	1.02	0.86	20	**Calculated**	0.011047
					ANN	0.011137
0.57	0.53	1.01	1.05	1	**Calculated**	0.004443
					ANN	0.004390
0.71	0.73	0.88	0.91	33	**Calculated**	0.005663
					ANN	0.005570

Table 2: VCPI Values for Kenyan System Bus 10

The VCPI values in Table 2 indicate that in all the randomly selected cases the bus is stable even with the selected single contingencies. The ANN generated values also closely follow the power flow values to a very great extent. A comparison of a contingency on line 20 shows bus 10 stability drops with a relatively small increase in the total system real power loading even when the reactive power demand at the bus is reduced. This reinforces its classification as a weak bus.